USGS
science for a changing world

Examining Submarine Ground-Water Discharge into Florida Bay by using ^{222}Rn and Continuous Resistivity Profiling

By Peter Swarzenski, Chris Reich, and David Rudnick

Prepared in cooperation with South Florida Water Management District

Open-File Report 2008–1342

U.S. Department of the Interior
U.S. Geological Survey

U.S. Department of the Interior
KEN SALAZAR, Secretary

U.S. Geological Survey
Suzette M. Kimball, Acting Director

U.S. Geological Survey, Reston, Virginia 2009

For product and ordering information:
World Wide Web: http://www.usgs.gov/pubprod
Telephone: 1-888-ASK-USGS

For more information on the USGS—the Federal source for science about the Earth,
its natural and living resources, natural hazards, and the environment:
World Wide Web: http://www.usgs.gov
Telephone: 1-888-ASK-USGS

Suggested citation:
Swarzenski, Peter, Reich, Chris, and Rudnick, David, 2009, Examining submarine ground-water discharge into Florida Bay by using ^{222}Rn and continuous resistivity profiling: U.S. Geological Survey Open-File Report 2008-1342, 66 p. [http://pubs.usgs.gov/of/2008/1342/].

Contents

Abstract 1

Introduction 2

Background 4

Methodology 7

Rn-222 surveys 7

Rn-222 time-series 8

Electromagnetic (EM) seepmeter 9

Marine resistivity 9

Results and Discussion 10

Rn-222 surveys 10

Rn-222 time-series 11

Key Largo Ranger Station (KLR) 11

Shell Key 12

Little Madeira Bay 13

Little Blackwater Sound 14

Radon Measurements and SGD Fluxes 15

EM seepmeter 17

SGD and Nutrients 18

Electrical resistivity in sediments 18

May 2007 19

September 2007 20

March 2008 23

Acknowledgments- 25

References 26

Figures

Figure 1. May 2007 ^{222}Rn survey (dpm L^{-1})..... 10

Figure 2. September 2007 ^{222}Rn survey (dpm L^{-1})..... 10

Figure 3. March 2008 ^{222}Rn survey (dpm L^{-1}). 10

Figure 4. Site map within Florida Bay, showing location of time-series and electromagentic (EM) seepmeter sites. 1-Little Madeira Bay, 2- Shell Key, 3- Key Largo Ranger Station, and 4-Little Blackwater Sound.... 12

Figure 5. May 2007 time-series water levels (dashed blue line; m), wind speed (solid grey line; m s^{-1}), specific conductivity (mS cm^{-1}), and temperature (^{o}C)..... 12

Figure 6. May 2007 time-series water levels (m) and surface water (sw) ^{222}Rn (dpm m^{-3})..... 12

Figure 7. September 2007 time-series water levels (dashed blue line; m), wind speed (solid grey line; m s^{-1}), specific conductivity (mS cm^{-1}), and temperature (^{o}C)..... 12

Figure 8. September 2007 time-series water levels (m) and surface water (sw) ^{222}Rn (dpm m^{-3})..... 12

Figure 9. March 2008 time-series water levels(dashed blue line; m), wind speed (solid grey line; m s^{-1}), specific conductivity (mS cm^{-1}), and temperature (^{o}C)..... 12

Figure 10. March 2008 time-series water levels (m) and surface water (sw) ^{222}Rn (dpm m^{-3}). 12

Figure 11. May 2007 time-series water levels(dashed blue line; m), wind speed (solid grey line; m s^{-1}), specific conductivity (mS cm^{-1}), and temperature (^{o}C)..... 13

Figure 12. May 2007 time-series water levels (m) and surface water (sw) ^{222}Rn (dpm m^{-3})..... 13

Figure 13. March 2008 time-series water levels (dashed blue line; m), wind speed (solid grey line; m s^{-1}), specific conductivity (mS cm^{-1}), and temperature (^{o}C)..... 13

Figure 14. March 2008 time-series water levels (m) and surface water (sw) ^{222}Rn (dpm m^{-3}). 13

Figure 15. May 2007 time-series water levels (dashed blue line; m), wind speed (solid grey line; m s^{-1}), specific conductivity (mS cm^{-1}), and temperature (^{o}C). 14
Figure 16. May 2007 time-series water levels (m) and surface water (sw) ^{222}Rn (dpm m^{-3}) 14
Figure 17. March 2008 time-series water levels (dashed blue line; m), wind speed (solid grey line; m s^{-1}), specific conductivity (mS cm^{-1}), and temperature (^{o}C). 14
Figure 18. March 2008 time-series water levels (m) and surface water (sw) ^{222}Rn (dpm m^{-3}). 14
Figure 19. September 2007 time-series water levels (dashed blue line; m), wind speed (solid grey line; m s^{-1}), specific conductivity (mS cm^{-1}), and temperature (^{o}C). 15
Figure 20. September 2007 time-series water levels (m) and surface water (sw) ^{222}Rn (dpm m^{-3}). 15
Figure 21. Electromagnetic (EM) seepmeter results during May, 2007 18
Figure 22. Map showing location of resistivity profiles for Buttonwood Bay-Key Largo and Blackwater Section 1.. 20
Figure 23. Profile of resistivity behind Key Largo in Buttonwood Sound collected on May 2007. Profile shows hummocky nature of subsurface (dashed white line). White line near surface is seafloor. 20
Figure 24. Profile of resistivity along eastern shore of Florida Bay, opposite to Blackwater Sound. Dip in dashed white line may be representative of lithologic variability. White line near surface is seafloor. 20
Figure 25. Map showing the resistivity survey area for September 2007. Map shows the CRP lines and breakdown of individual resistivity profiles. 20
Figure 26. Topography of the Q3 unconformity showing the northern keys high (Multer et al. 2002). 21
Figure 27. Resistivity profile from east of Porjoe Key west to the east side of Lake Key. It appears as though there is a high in the resistivity data that may correspond to a geologic high known as the Northern Keys High (Multer et al., 2002). 21
Figure 28. Resistivity profile from Little Blackwater Sound in the north to near Key Largo in Blackwater Sound. Dip in resistivity unit possibly representative of geologic low in the middle of Blackwater Sound and then shallowing again on the backside of Key Largo. 22

Figure 29. Resistivity section from the southern entrance to Little Blackwater Sound north just offshore the radon time-series location toward the mangrove land that rims the western edge of Little Blackwater Sound. Increase in resistivity could either be a result of 'fresher' water from the mangrove island to the west or a shallowing of a lithologic unit. 22

Figure 30. Back side of Key Largo. Low resistivity responding to marine water infilled limestone with no variability 22

Figure 31. Manatee Bay showing higher resistivity than that found along the backside of Key largo (FigZ1). The higher resistivity is most likely a response to lower salinity porewaters. 23

Figure 32. March 2008 boat surveys and respective CRP lines. 23

Figure 33. Image of measured (raw) apparent resistivity showing a shift in data between two consecutive data points. It is unknown what causes this immediate shift. 24

Figure 34. March 2008 CRP profile from within the entrance to C-111 canal out into Manatee Bay. Profile is typical of previous profiles taken within Manatee Bay. Numerous errors occurred at the beginning of the line which is now blanked out with the gray boxes. 24

Figure 35. March 2008 CRP profile along the backside of Key Largo in Blackwater Sound. Low resistivity values represent the groundwater exchange of marine salinity due to tidal pumping as well as the representation of slight changes in lithologic composition. 24

Tables

Table 1. Rn-derived SGD rates (cm d^{-1}) at the time-series stations within our study site. See Figure 4 for location information.....17

Conversion Factors

SI to Inch/Pound

Multiply	By	To obtain
	Length	
centimeter (cm)	0.3937	inch (in.)
kilometer (km)	0.5400	mile, nautical (nmi)
	Radioactivity	
becquerel per liter (Bq/L)	27.027	picocurie per liter (pCi/L)

Temperature in degrees Celsius (°C) may be converted to degrees Fahrenheit (°F) as follows:

°F=(1.8×°C)+32

Temperature in degrees Fahrenheit (°F) may be converted to degrees Celsius (°C) as follows:

°C=(°F-32)/1.8

Vertical coordinate information is referenced to the insert datum name (and abbreviation) here, for instance, “North American Vertical Datum of 1988 (NAVD 88)”

Horizontal coordinate information is referenced to the insert datum name (and abbreviation) here, for instance, “North American Datum of 1983 (NAD 83)”

Altitude, as used in this report, refers to distance above the vertical datum.

Specific conductance is given in microsiemens per centimeter at 25 degrees Celsius (µS/cm at 25°C).

This page intentionally left blank

Examining Submarine Ground-Water Discharge into Florida Bay by using ^{222}Rn and Continuous Resistivity Profiling

By Peter Swarzenski, Chris Reich, and David Rudnick

Abstract

Estimates of submarine ground-water discharge (SGD) into Florida Bay remain one of the least understood components of a regional water balance. To quantify the magnitude and seasonality of SGD into upper Florida Bay, research activities included the use of the natural geochemical tracer, ^{222}Rn, to examine potential SGD hotspots (^{222}Rn surveys) and to quantify the total (saline + fresh water component) SGD rates at select sites (^{222}Rn time-series). To obtain a synoptic map of the ^{222}Rn distribution within our study site in Florida Bay, we set up a flow-through system on a small boat that consisted of a Differential Global Positioning System, a calibrated YSI, Inc CTD sensor with a sampling rate of 0.5 min, and a submersible pump (z = 0.5 m) that continuously fed water into an air/water exchanger that was plumbed simultaneously into four RAD7 ^{222}Rn air monitors. To obtain local advective ground-water flux estimates, ^{222}Rn time-series experiments were deployed at strategic positions across hydrologic and geologic gradients within our study site. These time-series stations consisted of a submersible pump, a Solinist DIVER (to record continuous CTD parameters) and two RAD7 ^{222}Rn air monitors plumbed into an air/water exchanger. Repeat time-series ^{222}Rn measurements

were conducted for 3-4 days across several tidal excursions. Radon was also measured in the air during each sampling campaign by a dedicated RAD7. We obtained ground-water discharge information by calculating a ^{222}Rn mass balance that accounted for lateral and horizontal exchange, as well as an appropriate ground-water ^{222}Rn end member activity.

Another research component utilized marine continuous resistivity profiling (CRP) surveys to examine the subsurface salinity structure within Florida Bay sediments. This system consisted of an AGI SuperSting 8 channel receiver attached to a streamer cable that had two current (A,B) electrodes and nine potential electrodes that were spaced 10 m apart. A separate DGPS continuously sent position information to the SuperSting.

Results indicate that the ^{222}Rn maps provide a useful gauge of relative ground-water discharge into upper Florida Bay. The ^{222}Rn time-series measurements provide a reasonable estimate of site-specific total (saline and fresh) ground-water discharge (mean = 12.5±11.8 cm d^{-1}), while the saline nature of the shallow ground-water at our study site, as evidenced by CPR results, indicates that most of this discharge must be recycled sea water. The CRP data show some interesting trends that appear to be consistent with subsurface geologic and hydrologic characterization. For example, some of the highest resistivity (electrical conductivity^{-1}) values were recorded where one would expect a slight subsurface freshening (for example bayside Key Largo, or below the C111 canal).

Introduction

Submarine ground-water discharge (SGD) is a widely overlooked source term for some dissolved constituents as they make their way to the nearshore marine environment (Burnett et al. 2001a,b, 2003a, b, 2006; Moore, 1996, 1999; Slomp and Van Cappellen, 2004; Swarzenski, 2004a, 2007; Taniguchi et al., 2002, 2006). Almost twenty years ago Johannes (1980) inferred that SGD could

have a potential significance in coastal biological production and eutrophication. However, most often the only available estimate for local SGD rates are based on regional hydrologic characterization, and such data have generally produced widely-fluctuating SGD estimates. Even where ground-water flux estimates may be low, nutrient and/or contaminant loading could still be high depending upon the relative concentrations in the groundwater and overlying sea water. This is particularly true near urbanized coastlines, where anthropogenic changes in the quantity and quality of ground water may be directly translated to the nearshore marine environment by SGD, and where highly permeable strata underlie the coastal region, because local runoff may be relatively low and SGD can greatly exceed the terrestrial flow from adjacent rivers (Price et al., 2003; Swarzenski and Kindinger 2003). One such example is the highly transmissive Biscayne and Floridan aquifer system of south Florida (Corbett et al., 1999, 2000; Top et al., 2001; Chanton et al., 2003).

The rate of SGD is regulated in part by the hydraulic gradient between the aquifer and the overlying sea water, and it is maintained by natural recharge-discharge characteristics that can be modified by human water-supply and water-use requirements. Ground-water pumping in many coastal areas has resulted in substantial decreases in the potentiometric head (i.e., the level to which a column of water will rise in a tightly cased well drilled into the aquifer), thereby causing infiltration of sea water into coastal aquifers. Sea level rise, whether due to natural (glacio-eustasy) or anthropogenic causes, will result in additional increased landward flow of sea water into many coastal aquifers.

There are at least four major SGD pathways (Li et al., 1999; Swarzenski and Kindinger, 2003; Michael et al., 2003, 2005; Porcelli and Swarzenski, 2003; Weinstein et al., 2007): (1) diffuse seepage through nearshore sediments from a surficial aquifer; (2) focused submarine spring flow from deeper, more confined aquifers; (3) specific “point source” seepage through offshore sediments; and (4) ephemeral seepage due to tidal or wind-driven pumping in shallower waters. These processes can

release either freshwater or recycled sea water, as well as their associated dissolved constituents, to the nearshore marine environment. For example, the concentration of certain nitrogen and phosphorus species are typically much higher in ground water than in surface water (Price et al., 2003; Swarzenski et al., 2006b, 2007a,b; Kroeger et al., 2007). Some of these dissolved constituents may be artificially enhanced by anthropogenic activities and may ultimately discharge through SGD to nearshore marine environments where they may adversely impact nearshore marine ecosystems. Valiela et al. (1990) correlated fin and shellfish kills in several New England bays to eutrophication of ground water arising from borne nutrients. In this system, the authors suggest that the elevated nutrient levels were a function of sewage-contaminated groundwater and surface water. Capone and Bautista (1985) showed that a large component of the nearshore nitrogen cycle may be influenced by SGD processes. Similar studies have documented the importance of SGD in south Florida and the Florida Keys (Lapointe et al. 1990, Swarzenski et al., 2004c), Australia (Johannes, 1980), Gulf of Aqaba (Shellenbarger et al., 2006) and along the south Atlantic Bight (Moore, 1996).

Background

Florida Bay is a shallow bay south of peninsular Florida and north of the Florida Keys, and it constitutes an important component of the Comprehensive Everglades Restoration Plan (CERP). Florida Bay receives much of the runoff from the Everglades and from the rapidly developing south Florida landscape. Past development of south Florida's water resources likely influences current conditions, and future development and management of Florida's water resources, including both the water-use and ecosystem-restoration elements of CERP, will likely continue to impact future flows. Consequently, hydrodynamic and ecosystem models are critical to facilitating an understanding of both past and future conditions.

Existing hydrodynamic models of Florida Bay (e.g., HYCOM and others) currently do not account for SGD, though there is strong evidence to suggest that SGD does occur (Corbett et al., 1999, 2000; Swarzenski et al., 1999; Top et al. 2001; Price et al., 2003). Quantifying an SGD component in such numerical models may be complicated because: (1) ground-water salinity is often similar to surface- water salinity in Florida Bay; (2) ground-water discharge into Florida Bay may be balanced by a transfer of sea water into the underlying aquifer, which would result in a net zero exchange of water across the sediment/water interface, or (3) the models are incorrectly parameterized in other ways (for example, increased surface-water inflows, or incorrect evapotranspiration term). Although these models can approximate salinity in Florida Bay without SGD, these models cannot adequately address this primary objective unless SGD and sea water-groundwater exchange dynamics are adequately quantified and understood.

Current estimates of SGD to Florida Bay vary over an order of magnitude. Geochemical-tracer studies have reported values ranging from 0.8 to 16 cm d^{-1}, depending upon the particular tracer used. Direct measurement of the SGD rates made by using seepage meters have produced values ranging from 2 to 40 cm d^{-1} (Corbett et al., 1999, 2000). The geochemical-tracer studies have often used the deeper aquifers, such as the Hawthorn Group, the "River of Sand", and the Floridan aquifer, as the source of the SGD (e.g., Corbett et al., 1999, 2000; Top et al., 2001). However, these deeper aquifers are not the most likely sources of the SGD. Both the Hawthorn Group and the River of Sand (which is most likely a part of the Hawthorn Group) have low permeability. Groundwater from the Hawthorn Group has been shown to migrate to the bottom of the surficial aquifer system, but only diffusively (Price et al., 2003). The top of the Floridan aquifer is confined 250 - 300 m below Florida Bay. If the top of the aquifer were to be penetrated by a fault or fracture so that groundwater could migrate unimpeded to Florida Bay, an obvious "boil" of water would be observed. Such boils are currently observed off the coast of

Crescent Beach, Florida (Swarzenski et al., 2001) and at the Mud Hole Springs, in the eastern Gulf of Mexico. SGD into Florida Bay is more likely from shallow sources, with most of it characterized as recycled sea water (Swarzenski et al., 1999).

Regardless of the original sources, the ground water likely contains significant concentrations of nutrients that can then be transported to the sediments and overlying sea water to be utilized by seagrasses and other biological communities within Florida Bay. Ground-water concentrations of nitrogen and phosphorus are often higher than those in surface-waters (Price et al., 2006). Corbett et al. (1999) found that ground-water flux of nitrogen (110±60 mmol m^{-2} yr^{-1}) and phosphorus (0.21±0.11 mmol m^{-2} yr^{-1}) to Florida Bay may be comparable to surface-water flux of nitrogen and phosphorus to Florida Bay from the adjacent Everglades.

However, Corbett et al. (1999) cautioned that ground-water and nutrient fluxes are not uniform in space or time, but rather are likely controlled by a variety of spatial factors, such as the proximity to the mainland and the Florida Keys, and temporal factors, such as seasonal and/or tidal changes in the hydraulic gradients between the bay and the underlying aquifer. For instance, SGD along the northern coastline of Florida Bay is brackish and most likely seasonally driven by differences in water levels on either side of the Buttonwood embankment. Price et al. (2006) have shown that the brackish groundwater in this region is elevated in phosphorus, and that the phosphorus concentrations are positively correlated with salinity. Along the Florida Keys, differences in surface-water levels between Florida Bay and the Atlantic Ocean drive ground water back and forth beneath the Florida Keys. Some of the highest flux rates of ground-water discharge in response to this tidal cycling have been observed along the Florida Bay side of the northern Florida Keys (Corbett et al., 1999). This ground-water is most likely a mixture of Atlantic and Florida Bay water, though some freshwater associated with a ground-water lens in the Florida Keys may also contribute to this flow. Ground water discharge in the

central part of the bay is most likely driven by hypersaline conditions that often occur during the spring and summer months. In central Florida Bay, ground water often has salinities greater than 35 (Corbett et al., 1999; Swarzenski et al., 1999). The source of this high salinity groundwater is most likely surface water in the bay that has become hyper saline in the summer months. This dense, hyper saline water migrates as fingers into the sediments, thereby displacing less dense fresh or brackish groundwater in a process known as reflux. This less dense water may then discharge upward to the surface water carrying elevated concentrations of nutrients that are common to the Florida Bay sediments. This density-driven mechanism is most likely slow and seasonally driven.

Research activities for this project included two parts. The first research component involved the use of geochemical tracers (^{222}Rn) to examine potential SGD hotspots (^{222}Rn surveys) and to quantify total (saline + fresh water component) SGD rates at select sites from time-series ^{222}Rn measurements. The second research component utilized marine continuous resistivity (CRP) surveys to examine the subsurface salinity structure within Florida Bay sediments.

Methodology

Rn-222 Surveys

In May 2007, September 2007, and March 2008, a small boat (traveling at ~3-4 knots) was used in the three Florida Bay ^{222}Rn surveys to target potential seasonal variations in SGD. A submersible pump extending 0.5 m below the sea surface provided a continuous stream of water for the ^{222}Rn measurements. This water stream was fed at a rate of ~5 L min^{-1} into an air/water exchanger that was plumbed in parallel into four RAD7 ^{222}Rn detectors. If the water temperature is known, an air/water partition coefficient can be used to easily convert air ^{222}Rn measurements into water ^{222}Rn

measurements (Burnett et al., 2003b; Burnett and Dulaiova, 2003; Dulaiova et al., 2005, 2006; Swarzenski et al., 2007b, Swarzenski, 2007). Prior to entering the RAD7 detectors, the continuous air stream is run through a desiccant-filled column to remove excess moisture. In this configuration, the four RAD7s provide a new ^{222}Rn value every 10 min. An in place CTD mounted onto the submersible pump was used to collect continuous water-column parameters (i.e., salinity, pH, dissolved oxygen, and temperature), and a dedicated GPS instrument was used to collect real-time position and water-depth data.

Rn-222 Time-Series

Four-to-five day ^{222}Rn time-series experiments were conducted at the Key Largo Ranger Station (May 2007, September 2007, and March 2008), Shell Key (May 2007 and March 2008), Little Madeira Bay (May 2007 and March 2008), and Little Black Water (September 2007). The site of the Key Largo Ranger Station was just offshore from the main dock in about 1 m of water. The Shell Key site was sampled from a small tender anchored in about 0.5 m of water. Little Madeira Bay was sampled from the small island at the mouth of Little Madeira Bay (May 2007) and from the USGS gaging station located within the mouth of Taylor Slough (March 2008). Little Black Water was again sampled from a small tender, anchored off of a protecting mangrove fringe in about 1 m of water.

Each water column time-series ^{222}Rn station consisted of a submersible pump that provided well-mixed bottom water (for the purposes of these calculations the shallow nature of the time-series sites precludes significant stratification) to a air/water exchanger that was routed to two RAD7 ^{222}Rn detectors. Bottom water-column salinity, temperature, and depth were also simultaneously monitored with either YSI CTDs or Solinst LEVELOGGERS. Air from the exchanger was recycled through a radon-in-air monitoring system RAD7 (Durridge Co., Inc.) at a rate of ~ 1 L min^{-1} (Burnett et al.,

2001b). The RAD7 measures the activity of ^{218}Po ($t_{1/2}$ = 3.11 min), which is allowed to grow into equilibrium with its direct parent ^{222}Rn. To achieve equilibration and acceptable statistical counting results, the measurements were integrated over 30 min intervals. The ^{222}Rn concentration in water can then be calculated from the radon activity in air by using a temperature-dependent equilibrium equation (cf. Burnett and Dulaiova, 2003; Swarzenski, 2007). How a time-series of aqueous ^{222}Rn concentrations can be used to derive an SGD rate is discussed in Section 4.3.

Electromagnetic Seepmeter

During May 2007, an electromagnetic (EM) seepmeter (Swarzenski et al., 2004b) was installed for about 4 days, at the Key Largo Ranger Station. The EM seepmeter, which has a footprint of about 1 m, records the bi-directional (positive = discharge; negative = recharge) flow across the sediment/water interface every minute. The EM seepmeter was deployed on a sandy sea floor with its bottom rim inserted about 10 cm into the sediment.

Marine Resistivity

The use of electrical resistivity to examine the fresh water/salt water interface is well established (Swarzenski et al., 2007a) and has been improved by recent advances in streamer configuration, as well as in data acquisition and processing firmware and software (Swarzenski et al., 2006a, 2007b). In Florida Bay, CRP surveys were conducted concurrently with the ^{222}Rn surveys. In continuous marine mode, the 120 m cable that consists of two current and nine potential electrodes is pulled at a speed of ~3-4 knots on the surface of the water column. Real-time GPS data is simultaneously streamed into a SuperSting receiver. Styrofoam floats between each electrode keep the cable positively buoyant. Real-

time continuous water column salinity/temperature measurements were recorded on an YSI multimeter while water depth and the ship's position were recorded on a separate GPS instrument.

Results and Discussion

Rn-222 Surveys

Florida Bay was too rough for a bay-wide survey during May 2007, therefore, only a short transect behind a protecting mangrove fringe was conducted (fig. 1). Rn-222 concentrations were highest (>7 dpm L^{-1}) just bayside of Key Largo and decreased to below 2 dpm L^{-1} in the northerly part of the transect. During the September 2007 survey, ^{222}Rn concentrations ranged from 1.13 to 9.15 dpm L^{-1}, and most of the elevated ^{222}Rn values occurred either off bayside Key Largo or along the northern fringe of Florida Bay extending away from Little Madeira Bay (fig. 2). No ^{222}Rn anomalies were observed either north or east of Blackwater Sound during this survey. The March 2008 survey (fig. 3) recorded ^{222}Rn values that were generally lower in magnitude compared to the two previous surveys (0.4–7 dpm L^{-1}), with highest values again observed off Key Largo (Rock Harbor) and also just bayward of the C-111 canal.

Figure 1. May 2007 ^{222}Rn survey (dpm L^{-1}).

Figure 2. September 2007 ^{222}Rn survey (dpm L^{-1}).

Figure 3. March 2008 ^{222}Rn survey (dpm L^{-1}).

Rn-222 Time-Series

Key Largo Ranger Station

All of the time-series sites discussed below are identified in figure 4. The May 2008 Key Largo Ranger Station (KLR) station time-series data are show in figure 5. Water levels (blue dashed line) decreased slightly (~ 0.2 m) during the 4 day time-series, while wind speed (gray solid line; m s^{-1}), specific conductivity (mS cm^{-1}) and temperature (^{o}C) varied little. figure 6 shows time-series ^{222}Rn, which gradually increased in concentration from a low of about 15,000 dpm m^{-3} to more than 35,000 dpm m^{-3}. The variability in ^{222}Rn during the 4-day time-series shows regular highs and lows, but they do not appear to coincide directly with local water-level variations. It is interesting to note the gradient in ^{222}Rn concentrations along a transect from the KLR Station towards the interior of Florida Bay, as evidenced in the ^{222}Rn surveys. Figure 7 shows water levels (blue dashed line ; m), wind speed (gray solid line; m s^{-1}), specific conductivity (mS cm^{-1}) and temperature (^{o}C) during the September 2007 time-series. About mid-way during this (fig. 8) time-series, ^{222}Rn values decreased abruptly from values approaching 15,000 dpm m^{-3} to less than 1000 dpm m^{-3}. This period of low ^{222}Rn could reflect heightened gas transfer across the air/sea interface as a result of a storm, lateral inputs of low ^{222}Rn water, or periods of low SGD. Since there were no coincident anomalies in the wind speed data or surface water ^{222}Rn imply that it is likely that we observed a short period of little or no SGD at the KLR station during this time-series. The water-level record shows a slight high during this time and may confirm this low SGD signal. The March 2008 (figs. 9 and 10) time-series indicate a consistent warming trend, while the water level and specific conductivity records show little change. Rn-222 values (10,000–22,500 dpm m^{-3}) show systematic declines and increases that are, again, not obviously coupled to local water-level variations.

Figure 4. Figure 4. Site map within Florida Bay, showing location of time-series and electromagentic (EM) seepmeter sites. 1-Little Madeira Bay, 2- Shell Key, 3- Key Largo Ranger Station, and 4-Little Blackwater Sound.

Figure 5. May 2007 time-series water levels (dashed blue line; m), wind speed (solid grey line; m s^{-1}), specific conductivity (mS cm^{-1}), and temperature (C).

Figure 6. May 2007 time-series water levels (m) and surface water (sw) ^{222}Rn (dpm m^{-3}).

Figure 7. September 2007 time-series water levels (dashed blue line; m), wind speed (solid grey line; m s^{-1}), specific conductivity (mS cm^{-1}), and temperature (C).

Figure 8. September 2007 time-series water levels (m) and surface water (sw) ^{222}Rn (dpm m^{-3}).

Figure 9. March 2008 time-series water levels(dashed blue line; m), wind speed (solid grey line; m s^{-1}), specific conductivity (mS cm^{-1}), and temperature (C).

Figure 10. March 2008 time-series water levels (m) and surface water (sw) ^{222}Rn (dpm m^{-3}).

Shell Key

The May 2007 time-series (fig. 11) shows a 0.2 m drop in water level mid-time-series that appears also in the specific-conductivity record. Wind speeds and water temperatures are constant and predictable, respectively, and do not appear to directly influence the ^{222}Rn distribution (fig. 12). Distinct ^{222}Rn peaks were observed at regular ~12 hr intervals, providing strong evidence for some tidal modulation of SGD at this site, as traced by ^{222}Rn. This observation is noteworthy because the lunar tidal amplitude is near zero at this site, and the temperature profile does not indicate similar periodicity.

The March 2008 time-series (fig. 13) shows a slight increase in water levels and a specific conductivity anomaly (maybe due to sediment on the sensor). However, figure 14 illustrates the water level control on ^{222}Rn concentrations; as water levels and temperature increased, the ^{222}Rn distribution generally decreased in spite of pronounced variability.

Figure 11. May 2007 time-series water levels(dashed blue line; m), wind speed (solid grey line; m s^{-1}), specific conductivity (mS cm^{-1}), and temperature (C).

Figure 12. May 2007 time-series water levels (m) and surface water (sw) ^{222}Rn (dpm m^{-3}).

Figure 13. March 2008 time-series water levels (dashed blue line; m), wind speed (solid grey line; m s^{-1}), specific conductivity (mS cm^{-1}), and temperature (C).

Figure 14. March 2008 time-series water levels (m) and surface water (sw) ^{222}Rn (dpm m^{-3}).

Little Madeira Bay

This site was located on the northern shore of an island at the mouth of Little Madeira Bay. At this protected site, water levels, wind speed, specific conductivity, and temperature varied little (fig. 15) during our May 21-22, 2007, time-series. At this site, the ^{222}Rn concentrations were generally low (4000 – 6000 dpm m^{-3}) and the distribution of radon (fig. 16) also varied only slightly. Because of the lack of a pronounced SGD signal at this site, we relocated the time-series station to the mouth of Taylor Slough in 2008 and attached our ^{222}Rn equipment to the existing USGS water gaging station. Taylor Slough discharged noticeably into Little Madeira Bay during our March 2008 deployment, so the ^{222}Rn time-series data should reflect both an SGD and a fluvial (i.e., baseflow) record. As expected, specific

conductivity was much lower at this site than at other time-series sites within the Florida bay (fig. 17). The 0.5 m drop in water level on March 4 resulted from a change in the height of the submersible pump. (Because there was an abundance of fine particulates on the sea floor) The cinder block-mounted pump on the sea floor was repositioned into the middle of the water column (~0.5 m from the sediment/water interface). Note that water levels remained constant for the remainder of the time-series, while specific conductivity gradually increased to above 34 mS cm^{-1}. The ^{222}Rn distribution shows one pronounced peak (up to 12,500 dpm m^{-3}) on May 6 from a mean of about 7,000 dpm m^{-3}
(fig. 18).

Figure 15. May 2007 time-series water levels (dashed blue line; m), wind speed (solid grey line; m s^{-1}), specific conductivity (mS cm^{-1}), and temperature (C).

Figure 16. May 2007 time-series water levels (m) and surface water (sw) ^{222}Rn (dpm m^{-3}).

Figure 17. March 2008 time-series water levels (dashed blue line; m), wind speed (solid grey line; m s^{-1}), specific conductivity (mS cm^{-1}), and temperature (C).

Figure 18. March 2008 time-series water levels (m) and surface water (sw) ^{222}Rn (dpm m^{-3}).

Little Blackwater Sound

The Little Blackwater Sound site was occupied during September 2007 and was located adjacent to a mangrove fringe in about 1 m of water. While the mangroves offered some protection to several of the other time-series sites, here the prevailing winds were from the southeast, exposing the ^{222}Rn tender to moderate wind/wave action. As has been observed previously, water levels gradually increased 0.2 m

during the 4-day duration (fig. 19). In contrast, specific conductivities (mS cm^{-1}) were noticeably low (high of ~40 mS cm^{-1}) and fell dramatically on the first day to values below 28 mS cm^{-1}. Figure 20 shows the corresponding ^{222}Rn record; values peaked (22,500 dpm m^{-3}) at the onset of time-series and then decreased almost exponentially to background values, except for one peak on September 5th. After September 5th there were no additional inputs of ^{222}Rn, implying that SGD was minimal during this part of our sampling time.

Figure 19. September 2007 time-series water levels (dashed blue line; m), wind speed (solid grey line; m s^{-1}), specific conductivity (mS cm^{-1}), and temperature (C).

Figure 20. September 2007 time-series water levels (m) and surface water (sw) ^{222}Rn (dpm m^{-3}).

Radon Measurements and SGD Fluxes

Excess ^{222}Rn activities in the water column were obtained by subtracting representative activities of its immediate radiogenic parent, ^{226}Ra (cf. Swarzenski et al., 1999; Chanton et al., 2003). Half-hour excess ^{222}Rn inventories (dpm m^{-2}) were calculated by multiplying the excess ^{222}Rn activity by the corresponding water-level data; they were then corrected for atmospheric-loss terms. Atmospheric evasion was calculated by using equations presented in MacIntyre et al. (1995), which derive gas exchange across the air/sea interface from a concentration gradient, as well as local temperature and wind speed. The local air ^{222}Rn activity, which never exceeded 200 dpm m^{-3} during all three sampling events, was measured continuously with a dedicated RAD7 during each of the sampling campaigns. Lateral mixing loss terms were obtained from the time-series ^{222}Rn measurements by examining the change in the measured excess inventories over time. A more complete review of the equations and

assumptions of the above approach can be found in Burnett and Dulaiova (2003), Swarzenski et al. (2006a, b, 2007b), and Swarzenski (2007)

To obtain an SGD rate from the ^{222}Rn flux calculations, one can simply divide by a representative ground-water ^{222}Rn activity. Corbett et al. (1999) used sediment-equilibration experiments and direct groundwater measurements (n=73) to obtain a mean groundwater ^{222}Rn value of 400 dpm L^{-1}. We confirmed this value with additional spot ground water ^{222}Rn measurements (n=9) collected from select wells in September 2007 using a RAD-H2O system.

Table 1 summarizes the calculated SGD rates for the three sampling events. Little Madeira Bay and Little Blackwater Sound had the lowest calculated SGD rates (mean ~5 cm d^{-1}), while Shell Key (mean ~10 cm d^{-1}) and Key Largo Ranger Station (mean ~21 cm d^{-1}) had higher rates. A mean ground-water discharge rate considering all sites is 12.5±11.8 cm d^{-1}, which deceases to 8.5±4.0 cm d^{-1} if we do not consider the elevated May 2007 data (40.2±22.6 cm d^{-1}). Such rates compare well with previous estimates of ground-water discharge into Florida Bay (Corbett et al., 1999, 2000; Top et al., Chanton et al., 2003). SGD in Florida Bay is expressed overwhelmingly as recirculated sea water that is driven largely by the Atlantic tidal stage in southern Florida Bay and, to a lesser extent, by local recharge (seasonality) along the northern bay. Because evaporation rates in the bay typically exceed recharge, a negative water balance supports salinization, and the groundwater is often hypersaline.

Table 1. ^{222}Rn-derived SGD rates (cm d^{-1}) at the time-series stations within the study site, Florida Bay. [See figure 4 for location information.]

Date	Key Largo Ranger Station	Shell Key	Little Madeira	Little Blackwater
		(cm d^{-1})		
May 2007	40.2±22.6 (168*)	13.9±7.2 (90)	4.2±3.2 (87)[a]	---
September 2007	11.0±13.4 (195)	---	---	5.3±18.8 (194)
March 2008	12.8±11.4 (221)	7.4±6.9 (191)	5.2±6.6 (188)[b]	---

*Number in parentheses denotes number of samples
[a]Located at the entrance to Little Madeira Bay
[b]Located at the mouth of Taylor Slough

	All numbers (cm d^{-1})	w/o KLR May 2007 (cm d^{-1})
mean	12.5±11.8	8.5±4.0

Electromagnetic Seepmeter

Electromagnetic (EM) seepage at KLR during May 2007 is shown in figure 21. The local Atlantic tide (Virginia Key) is also plotted as a measure of the purported dominant local SGD driver. While there are obvious trends in the EM seepmeter data that follow some periodicity, it is not clear that Atlantic water level directly drives the EM-seepage fluctuations. At this site in May 2007, the ^{222}Rn time-series data measured anomalously large SGD rates (40.2±22.6 cm d^{-1}), although this rate is not above values observed previously (Corbett et al., 2000). It is possible that EM-seepmeter rates could be influenced by either physical (i.e., poor seal with the sediment) or hydrologic ("Bernoulli') effects, as well as by real localized flow patterns.

Figure 21. Electromagnetic seepmeter results during May 2007.

Surface Groundwater Data and Nutrients

Moore (1996, 1999) and other researchers (e.g. Slomp and Van Cappellen, 2004; Shellenbarger et al., 2006) suggested that SGD and, specifically, recirculated sea-water discharge could have a major impact on the chemical budget of coastal sea water and on its nutrient content. This study conducted in Florida Bay revealed that, while there is little fresh water being discharged into our study sites, there is consistent upward flow of recirculated sea water, and it is known that this newly exchanged water can be nutrient rich (cf. Price et al., 2003). Collaborators have examined the nutrient concentrations of this discharging water, and from our data we will be able to construct SGD nutrient-loading estimates into the bay that can then be compared to more traditional nutrient sources (i.e., atmospheric deposition and fluvial inputs).

Electrical Resistivity in Sediments

The use of electrical resistivity techniques to measure the resistivity (= electrical conductivity^{-1}) of coastal sediments and pore fluids has recently shown considerable advances (Swarzenski et al., 2004c, 2006a; 2007b). The resistivity method measures the apparent resistivity (ohm-m) of the subsurface geologic and hydrologic properties, including sediment type, bedrock fractures, porosity, temperature, and ground-water salinity (Swarzenski et al., 2006a, 2007a). Variations in electrical resistivity may indicate changes in the lithology or subsurface salinity field; under like geologic conditions, elevated apparent resistivity values correspond to freshened water masses that are less conductive. Electrical-resistivity systems are used in streaming mode to produce a continuous

resistivity profile (CRP) of coastal hydrologic processes. Detailed information on the heterogeneity of both the rock type and pore-fluid specific conductance (or salinity) is collected and stored on the AGI Supersting as an apparent measured resistivity. During data processing, the apparent resistivity is compared to a mathematical model and iterated until root mean square values are within predetermined limits.

Select CRP profiles for each of the sampling trips are discussed below. Weather conditions have a large impact on the quality of the data collected by the CRP system. Wave conditions cause electrodes to become exposed to the air, thereby causing errors and missing data. If conditions are severe enough, the resistivity system will shut down due to continuously repeated errors.

May 2007

CRP was conducted along the eastern shore of Florida Bay as weather conditions were not ideal for the operation of the system in any open-water areas. Easterly winds at 25-30 knots during the entire week allowed for the collection of only one day of CRP data. Approximately 30 km of data were collected on May 22, 2007; however, most of the data contain anomalies or are sparse due to wave conditions. Figure 22 shows the location of two short CRP profiles. Figure 23 shows a profile in Buttonwood Sound (north of Key Largo). The hummocky nature of the resistivity profile may represent karst-like subsurface features. A change in porosity or permeability would also result in a change in resistivity and may act as pathways for preferential exchange of groundwater and surface water. Determining whether or not these changes are caused by porosity or permeability may provide insight on locations of preferential exchange of groundwater and surface water. Other lithologic representations of heterogeneity in the bay can be seen by a sag in the resistivity midway along Blackwater Section 1 profile (fig. 24).

Figure 22. Map showing location of resistivity profiles for Buttonwood Bay-Key Largo and Blackwater Section 1.

Figure 23. Profile of resistivity behind Key Largo in Buttonwood Sound collected on May 2007. Profile shows hummocky nature of subsurface (dashed white line). White line near surface is seafloor.

Figure 24. Profile of resistivity along eastern shore of Florida Bay, opposite to Blackwater Sound. Dip in dashed white line may be representative of lithologic variability. White line near surface is seafloor.

September 2007

Weather conditions were much more amenable for CRP surveys during the wet seasons. Approximately 120 km of CRP data was collected in September 2007 over a period of 4 days. A very large area was surveyed that included: eastern sections of Florida Bay from along the northern shore to southern shore, Blackwater and Little Blackwater Sounds, Barnes Sound, and Manatee Bay (fig. 25).

Figure 25. Map showing the resistivity survey area for September 2007. Map shows the CRP lines and breakdown of individual resistivity profiles.

Two CRP surveys illustrate subsurface lithological units in Florida Bay. Based on geologic maps, there is an area through the middle section of Florida Bay where the Quaternary section is compressed. Multer et al. (2002) have summarized the core log data from Florida Bay and indicate that the top of the Q3 unit is shallower in the middle section of Florida Bay than it is beneath the Keys or in

western Florida Bay (fig. 26). The Q3 unconformity of south Florida, also called the Ft. Thompson Frm., consists of a limestone cap that can serve as a water-bearing unit in Florida Bay (Multer et al., 2002). The gradual shallowing of the Q3 is illustrated in figure 27 where a CRP line (Porjoe to Lake Key) runs from east to west from near Porjoe Key toward Lake Key. The more resistive unit is approximately 18 m below the seafloor on the eastern side where Multer et al. (2002) show the depth of the Q3 to be 12 m, rising to about 10 m below the sea floor just west of Nest Key. Multer et al. (2002) describe the Q3 coming up to ~6m west of Nest Key. Monitoring wells at both Nest and Lake Keys have shown near to slightly above marine salinity; therefore, the observed change in resistivity most likely represents a lithologic change.

Another example of the subsurface geologic structure discussed by Multer et al. (2002) may be seen in the Little Blackwater Sound to Key Largo CRP profile (fig. 28). The CRP profile shows the unit deepening to nearly 22 m below the sea floor in the middle of Blackwater Sound and then shallowing to around 18 m below the sea floor near Key Largo. The Little Blackwater Sound to Key Largo profile can be loosely correlated to the topographic contours of Multer and others (2002); for example, a deeper unit occurs beneath Blackwater Sound and shallows up on the bayside of Key Largo.

Figure 26. Topography of the Q3 unconformity showing the northern keys high (Multer et al. 2002).

Figure 27. Resistivity profile from east of Porjoe Key west to the east side of Lake Key. It appears as though there is a high in the resistivity data that may correspond to a geologic high known as the Northern Keys High (Multer et al., 2002).

Figure 28. Resistivity profile from Little Blackwater Sound in the north to near Key Largo in Blackwater Sound. Dip in resistivity unit possibly representative of geologic low in the middle of Blackwater Sound and then shallowing again on the backside of Key Largo.

The hydrologic influence may be assessed by comparing and contrasting CRP profiles from areas that receive direct freshwater influx versus those that are isolated by marine water. The Little Blackwater profile (fig. 29) shows a gradual increase in subsurface resistivity from the south to the north. The northern section near 6,700 m is close to land and near the radon time-series site mentioned earlier. The higher subsurface resistivity may be a result of slight freshening of pore waters from the recharge of rainfall on land and subsequent slow seepage outward into the bay. There are no wells in Little Blackwater to provide control on pore-water salinity, but surface-water salinity during the survey period ranged from 17 to 19 for Little Blackwater Sound. The surface-water salinity is most likely a result of surface freshwater releases from the Everglades to the north and is not a result of submarine ground-water discharge.

Figure 29. Resistivity section from the southern entrance to Little Blackwater Sound north just offshore the Radon time-series location toward the mangrove land that rims the western edge of Little Blackwater Sound. Increase in resistivity could either be a result of 'fresher' water from the mangrove island to the west or a shallowing of a lithologic unit.

Figure 30. Back side of Key Largo. Low resistivity to marine water infilled limestone resulting in little variability.

A comparison of Barnes Sound East and Manatee Bay North CRP profiles shows the influences of hydrology and pore-water salinity. The Barnes Sound East profile (fig. 30), locked along the back

side of Key Largo in Barnes Sound, contrasts with the Manatee Bay North profile (fig. 31) located along the northern shore near where C-111 canal exits. The subsurface-resistivity values are much higher for Manatee Bay as a result of near-continuous influx of freshwater along that portion of the coastline. Contrasting with Manatee Bay is Barnes Sound East, where tidal pumping drives the exchange of groundwater along the backside of Key Largo. The exchange of water near Key Largo is completely of marine origin, and salinities range from 33-40.

Figure 31. Manatee Bay showing higher resistivity than that found along the backside of Key largo (FigZ1). The higher resistivity is most likely a response to lower salinity porewaters.

March 2008

The March 2008 survey was an attempt to repeat the first dry season sampling run (May 2007) that was not fully completed due to high wind and rough seas. Conditions similar to those in May 2007 were encountered during the March 2008 trip, with winds from 15-20 kts and choppy bay waters. Rough water caused the AGI Supersting to shut down occasionally due to numerous errors caused by electrodes coming out of the water. Of the ~150 line kilometers surveyed, only about half contained useful resistivity data (Fig. 32). Typically, the resistivity system logs the entire time that the radon system is collecting data. However, due to the loss of the March 4 data, the unit was run only occasionally, and data was consistently downloaded onto a laptop computer.

Figure 32. March 2008 boat surveys and respective CRP lines.

Unfortunately, resistivity data from March 2008 are sparse and composed of numerous shifts, which is primarily a result of rough sea state. Shifts that do occur are random and can be found in many CRP profiles (see figure 33 for an example of a shift). Those profiles that do have clean data look similar to those measured in September 2007. It does not appear that there are any major changes in resistivity values between wet and dry seasons. For example, profiles from C-111 canal in Manatee Bay (fig. 34) and along the bayside of Key Largo in Blackwater Sound (fig. 35) show very similar profiles to those collected in September 2007 (figs 30 and 31): higher subsurface resistivity in the Manatee Bay area and low resistivity near Key Largo. The Key Largo profile (fig. 35) may correspond more to the lithologic change mentioned earlier (Q3 topography of Multer et al., 2002), and the C-111 profile may be more closely representative of pore-water salinity.

Figure 33. Image of measured (raw) apparent resistivity showing a shift in values between two consecutive data points. It is unknown what causes this shift.

Figure 34. March 2008 CRP profile from within the entrance to C-111 canal out into Manatee Bay. Profile is typical of previous profiles taken within Manatee Bay. Numerous errors occurred at the beginning of the line which is now blanked out with the gray boxes.

Figure 35. March 2008 CRP profile along the backside of Key Largo in Blackwater Sound. Low resistivity values represent the exchange of groundwater with marine salinity due to tidal pumping as well as the representation of slight changes in lithologic composition.

Acknowledgments

PWS wishes to thank the United States Geological Survey Coastal Marine and Geology Program for continued support in the field of SGD science. This project was supported, in part, by a grant from the South Florida Water Management District. Continued collaboration with Rene Price (FIU), as well as with Mark Rains (USF) and their respective students, is gratefully acknowledged. Marci Marot (USGS) and Christina Stringer (USF) provided expert field assistance.

References

Burnett, W.C., Aggarwal, P.K., Bokuniewicz, H., Cable, J.E., Charette, M.A., et al. 2006, Quantifying submarine groundwater discharge in the coastal zone via multiple methods. Science of the Total Environment 367, 498-543.

Burnett, W.C., Bokuniewicz, H., Huettel, M., Moore, W.S. and Taniguchi, M. 2003a, Groundwater and pore water inputs to the coastal zone: Biogeochemistry 66, 3-33.

Burnett, W.C., Cable, J.E. and Corbett, D.R., 2003b, Radon tracing of submarine groundwater discharge in coastal environments. In: Taniguchi, M., Wang, K., and Gamo, T. (Eds.), Land and Marine Hydrogeology. Elsevier Publications, pp. 25-43.

Burnett, W.C. and Dulaiova, H. 2003, estimating the dynamics of groundwater input into the coast zone via continuous radon-222 measurements, Environmental Radioactivity 69, 21-35.

Burnett, W.C., Kim, G. and Lane-Smith, D. 2001b, A continuous radon monitor for use in coastal ocean waters, Journal of Radioanalytical and Nuclear Chemistry 249, 167–172.

Burnett, W.C., Taniguchi, M. and Oberdorfer, J. 2001a, Measurement and significance of the direct discharge of groundwater in the coastal zone, Journal of Sea Research 46, 109-116.

Capone, D.G. and Bautista, M.F., 1985, A groundwater source of nitrate in nearshore marine sediments. Nature, 313, 214-216.

Chanton, J.P., Burnett, W.C., Dulaiova, H., Corbett, D.R. and Taniguchi, M. 2003, Seepage rate variability in Florida Bay driven by Atlantic tidal height. Biogeochemistry 66,187-202.

Corbett, R.D., Chanton, J., Burnett, W., Dillon, K. and Rutkowski, C. 1999, Patterns of groundwater discharge into Florida Bay. Limnology and Oceanography 44, 1045-1055.

Corbett, D.R., Dillon, K., Burnett, W.C. and Chanton, J.P., 2000, Estimating the groundwater contribution into Florida Bay via natural tracers, 222Rn and CH4. Limnology and Oceanography 45, 1546-1557.

Dulaiova, H., Peterson, R., Burnett, W.C. and Lane-Smith, D., 2005, A multidetector continuous monitor for assessment of 222Rn in the coastal ocean. Journal of Radioanalytical and Nuclear Chemistry 263, 361-365.

Dulaiova, H. and Burnett, W.C., 2006, Radon loss across the water / air interface estimated from 222Rn / 224Ra. Geophysical Research Letters 33, L05606. doi:10.1029/2005GL025023.

Dulaiova, H., Burnett, W.C., Chanton, J.P., Moore, W.S., Bokuniewicz, H.J., Charette, M.A. and Sholkovitz, E., 2006, Assessment of groundwater discharges into West Neck Bay, New York, via natural tracers. Continental Shelf Research 26, 1971-1983.

Johannes, R., 1980, The ecological significance of the submarine discharge of groundwater. Marine Ecology Progress Series, 3, 365–373.

Kroeger, K.D., Swarzenski, P.W., Reich, C. and Greenwood, W.J., 2007, Submarine groundwater discharge to Tampa Bay: nutrient fluxes and biogeochemistry of the coastal aquifer. Marine Chemistry 104, 85-97.

Lapointe, B.E., O'Connell, J.D. and Garrett, G.S., 1990, Nutrient couplings between onsite sewage disposal systems, groundwaters, and nearshore surface waters of the Florida Keys. Biogeochemistry 10, 289-307.

Li, L., Barry, D.A., Stagnitti, F. and Parlange, J.Y., 1999, Submarine groundwater discharge and associated chemical input to a coastal sea, Water Resources Research 35, 3253– 3259.

MacIntyre, S., Wanninkhof, R. and Chanton, J.P., 1995, Trace gas exchange in freshwater and coastal marine systems: flux across the air water interface. In, Methods in Ecology: Biogenic Trace Gases:

Measuring Emissions from Soil and Water, Eds. P. Matson and R. Harriss. Blackwell Scientific, pp 52-97.

Michael, H.A., Lubetsky, J.S. and Harvey, C.F., 2003, Characterizing submarine groundwater discharge: a seepage meter study in Waquoit Bay, Massachusetts, Geophysical Research Letters 30 1297, doi: 10.1029/2002GL016000.

Michael, H.A., Mulligan, A.E. and Harvey, C.F., 2005, Seasonal oscillations in water exchanger between aquifers and coastal ocean, Nature 436, 1145-1148.

Moore, W.S., 1996, Large groundwater inputs to coastal waters revealed by ^{226}Rn enrichments, Nature 380, 612–614.

Moore, W.S., 1999, The subterranean estuary: a reaction zone of ground water and sea water, Marine Chemistry 65, 111-125.

Multer, H.G., Gischler, E., Lundberg, J., Simmons, K.R. and Shinn, E.A., 2002, Key Largo Limestone revisited: Pleistocene shelf-edge facies, Florida Keys, USA: Facies 46: 229–272.

Porcelli, D. and Swarzenski, P.W., 2003, The behaviour of U- and Th series nuclides in groundwater and the tracing of groundwater. Reviews in Mineralogy and Geochemistry 52: 317-361.

Price, R.M., Top, Z., Happell, J.D. and Swart, P.K., 2003, Use of tritium and helium to define groundwater flow conditions in Everglades National Park. Water Resources Research, 39: 1267, doi:10.1029/2002WR001929.

Price, R.M., Swart, P.K. and Fourqurean, J.W., 2006, Coastal groundwater discharge-an additional source of phosphorus for the oligotrophic wetlands of the Everglades, Hydrobiologia, 569, 23-36. doi:10.1007/s10750-006-0120-5.

Shellenbarger, G.G., Monismith, S.G., Genin, A. and Paytan, A., 2006, The importance of submarine groundwater discharge to the nearshore nutrient supply in the Gulf of Aqaba (Israel), Limnology and Oceanography 51, 1876-1886.

Slomp, C.P. and Van Cappellen, P., 2004, Nutrient inputs to the coastal ocean through submarine groundwater discharge: controls and potential impact, Journal of Hydrology 295, 64-86.

Swarzenski, P.W., 2007, U/Th series radionuclides as tracers of coastal groundwater. Chemical Reviews 107(2), 663-674, doi: 10.1021/cr0503761

Swarzenski, P.W., Holmes, C.W., Shinn, E.A. and Moore, W.S., 1999, Tracing the mixing and movement of ground water into Florida Bay with four naturally occurring radium isotopes. In, Proc.1999 Georgia Water Resources Conference, Ed. K.J. Hatcher, Univ. of Georgia, pp.590-592.

Swarzenski, P.W., Reich, C.D., Spechler, R.M., Kindinger, J.L. and Moore, W.S., 2001, Using multiple geochemical tracers to characterize the hydrogeology of the submarine spring off Crescent Beach, Florida. Chemical Geology 179,187-202.

Swarzenski, P.W. and Kindinger, J.L., 2003, Leaky Coastal Margins: Examples of enhanced coastal groundwater/surface water exchange from Tampa Bay and Crescent Beach Submarine Spring, Florida, USA. In, Coastal Aquifer Management, Monitoring and Modeling and Case Studies. Eds A. Cheng and D. Ouazar. CRC/Lewis Press, pp 93-112.

Swarzenski P.W., Bratton, J. and Crusius, J., 2004a, Submarine groundwater discharge and its role in coastal processes and ecosystems. U.S. Geological Survey Open File Report 2204-1226.

Swarzenski, P.W., Charette, M. and Langevin, C., 2004b, An autonomous, electromagnetic seepage meter to study coastal groundwater/surface water exchange. U.S. Geological Survey Open File Report 2004-1369.

Swarzenski, P.W., Burnett, B., Reich, C., Dulaiova, H., Peterson, R. and Meunier, J., 2004c, Novel geophysical and geochemical techniques to study submarine groundwater discharge in Biscayne Bay, Fl. U.S. Geological Survey FS-2004-3117.

Swarzenski, P.W., Burnett W.C., Weinstein, Y., Greenwood, W.J., Herut, B., Peterson, R. and Dimova, N., 2006a, Combined time-series resistivity and geochemical tracer techniques to examine submarine groundwater discharge at Dor Beach Israel. Geophysical Research Letters, 33, L24405, doi:10.1029/2006GL028282.

Swarzenski, P.W., Orem, W.G., McPherson, B.F., Baskaran, M. and Wan, Y., 2006b, Biogeochemical transport in the Loxahatchee river estuary: the role of submarine groundwater discharge. Marine Chemistry 101, 248-265.

Swarzenski, P.W. Kruse, S. Reich, C. and Swarzenski, W.V., 2007a. Multi-channel resistivity investigations of the fresh water/saltwater interface: a new tool to study an old problem. In, A New Focus on Groundwater–Sea water Interactions. Eds W. Sanford, C. Langevin, M. Polemio, and P. Povinec. IAHS Publ. 312, 100-108.

Swarzenski, P.W., Simonds, F.W., Paulson, A. Kruse, S. and Reich, C. 2007b, A geochemical and geophysical examination of submarine groundwater discharge and associated nutrient loading estimates into Lynch Cove, Hood Canal, WA. Environmental Science and Technology 41, 7022-7029.

Taniguchi, M., Burnett, W.C., Cable, J.E., and Turner, J.V., 2002, Investigation of submarine groundwater discharge, Hydrological Processes 16, 2115-2129.

Taniguchi, M., Ishitobi, T. and Shimada, J., 2006, Dynamics of submarine groundwater discharge and freshwater-sea water interface, Journal of Geophysical Research 111, C01008, doi:10.1029/2005JC002924,

Top, Z., Brand, L.E., Corbett, R.D. Burnett, W. and Chanton, J.P, 2001, Helium and radon as tracers of groundwater input into Florida Bay. Journal of Coastal Research 17, 859-868.

Valiela, I., Costa, J., Foreman, K., Teal, J.M., Howes, B. and Aubrey, D., 1990, Transport of water-borne nutrients from watersheds and their effects on coastal waters. Biogeochemistry, 10, 177-198.

Weinstein, Y., Burnett, W. C., Swarzenski, P. W., Shalem, Y., Yechieli, Y. and Herut, B. 2007, Role of aquifer heterogeneity in fresh groundwater discharge and sea water recycling: An example from the Carmel coast, Israel, Journal of Geophysical Research 112, C12016, doi:10.1029/2007JC004112.

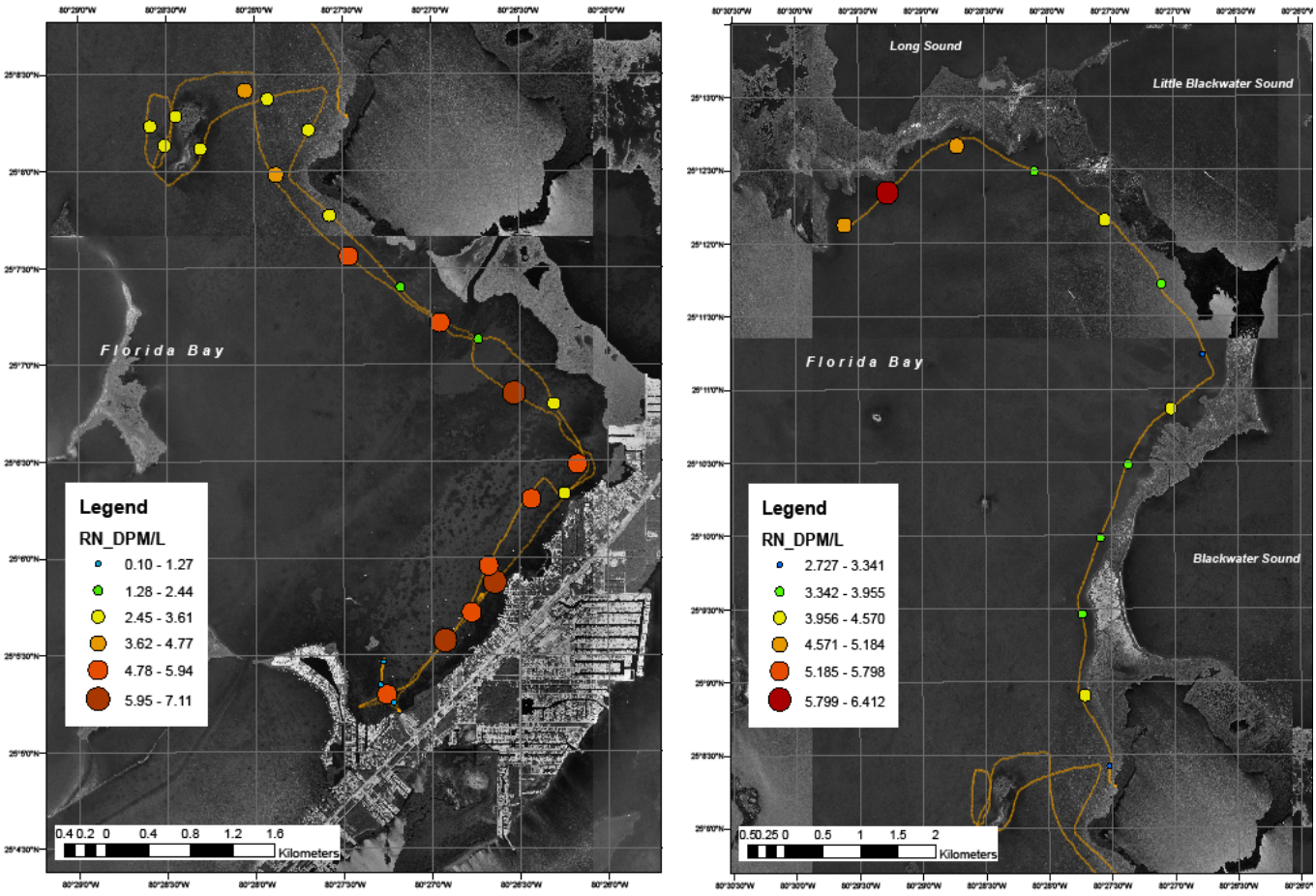

Figure 1. May 2007 ^{222}Rn survey (dpm L^{-1}), Florida Bay.

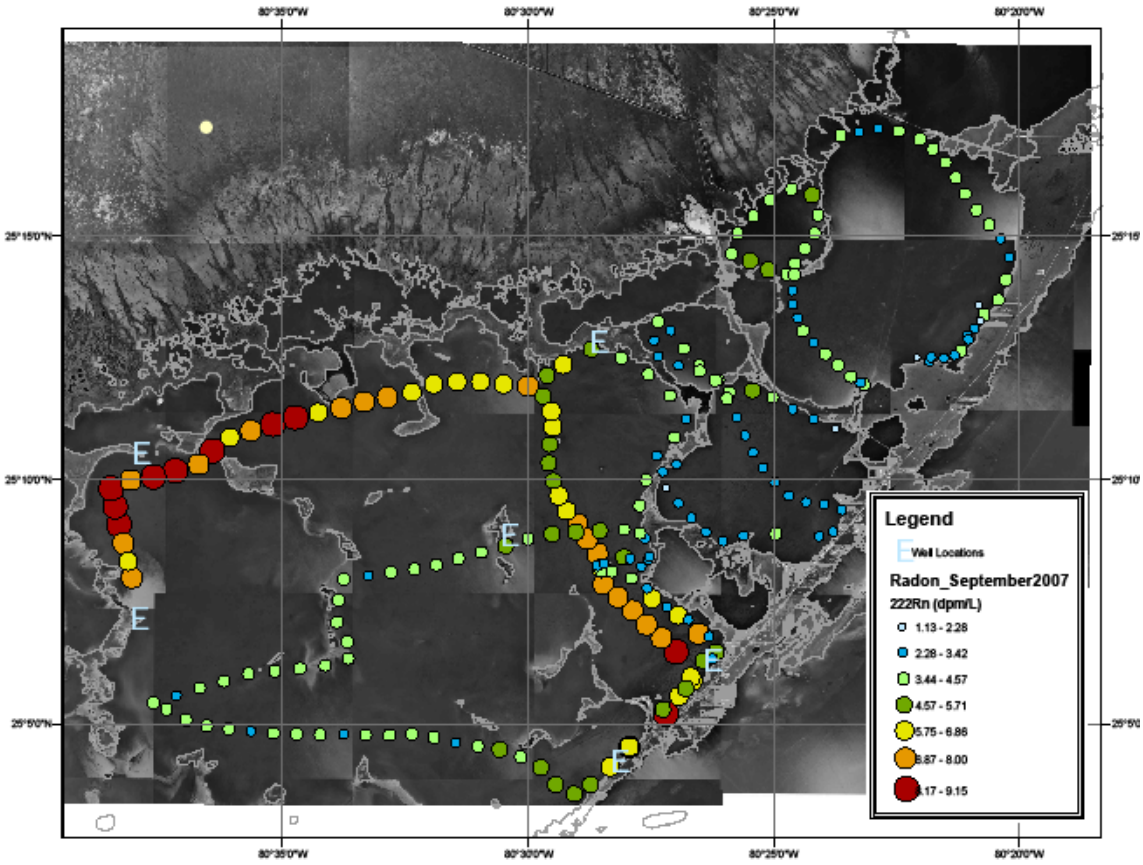

Figure 2. September 2007 ^{222}Rn survey (dpm L^{-1}), Florida Bay.

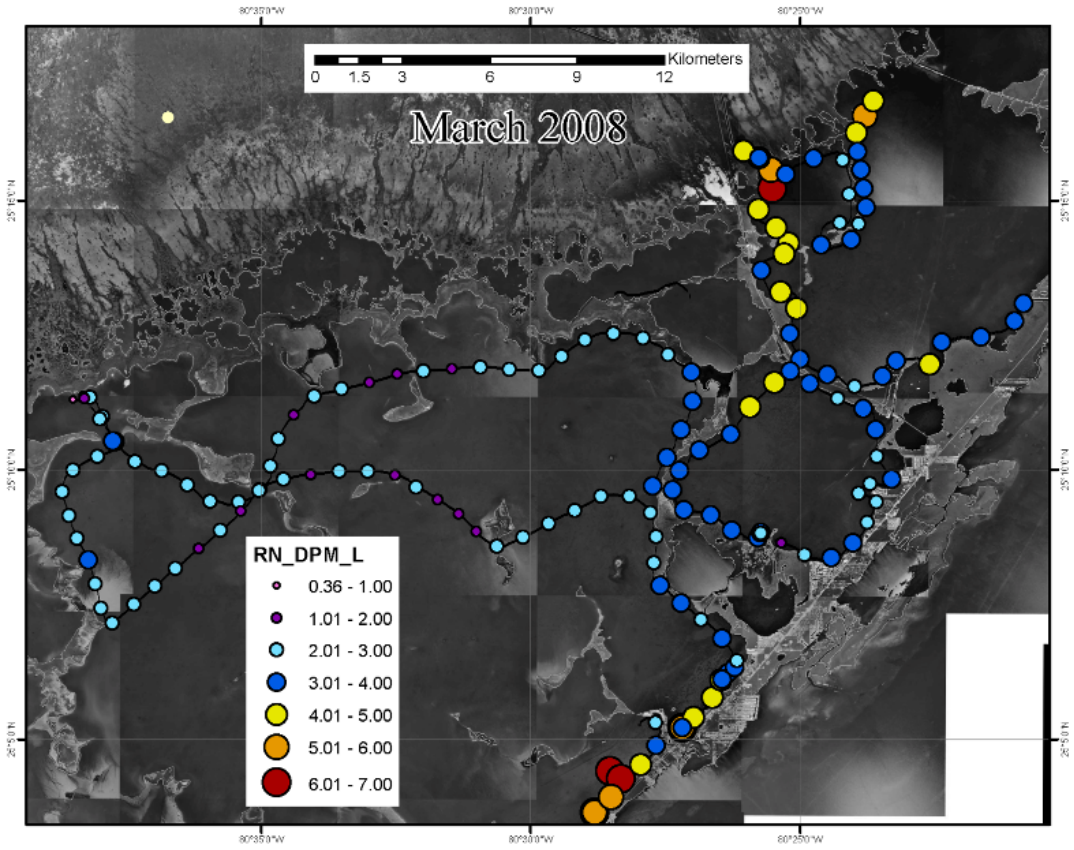

Figure 3. March 2008 ^{222}Rn survey (dpm L^{-1}), Florida Bay.

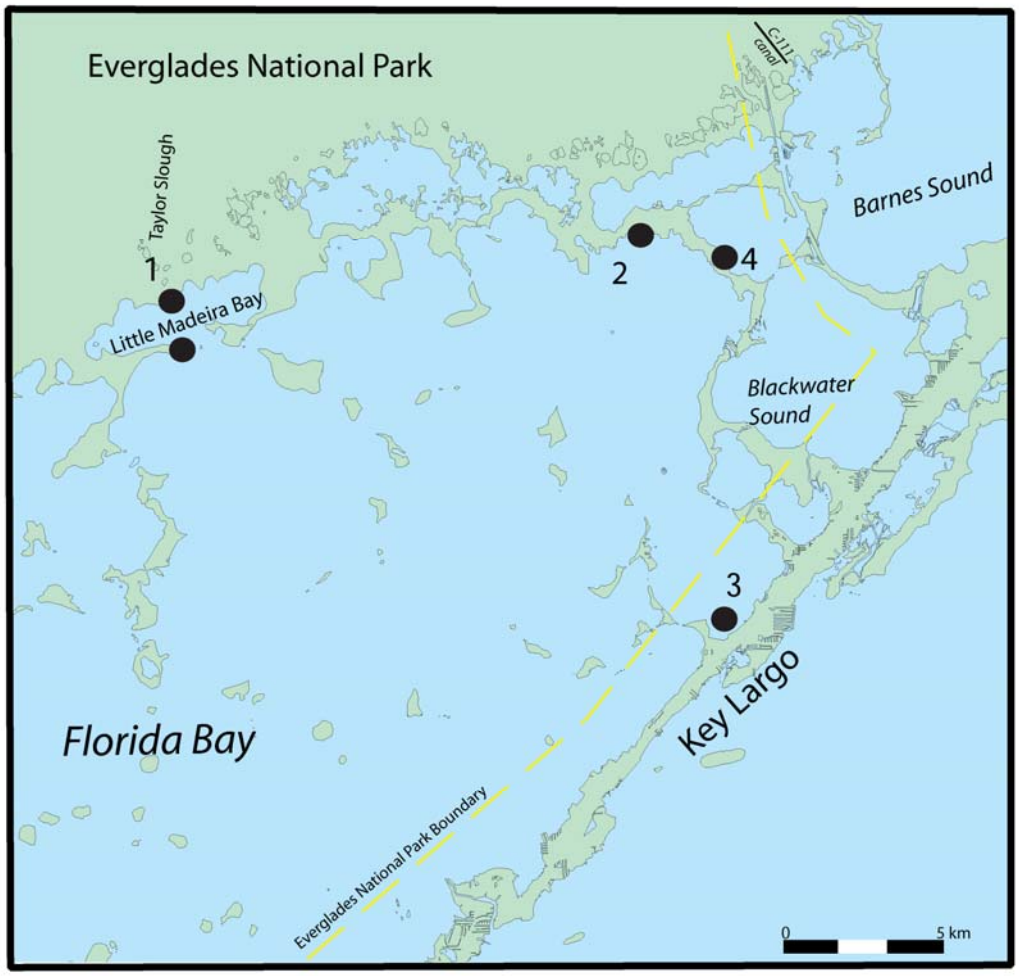

Figure 4. Site map within Florida Bay, showing location of time-series and electromagentic (EM) seepmeter sites, Florida Bay (1) Little Madeira Bay; (2) Shell Key; (3) Key Largo Ranger Station; and (4) Little Blackwater Sound.

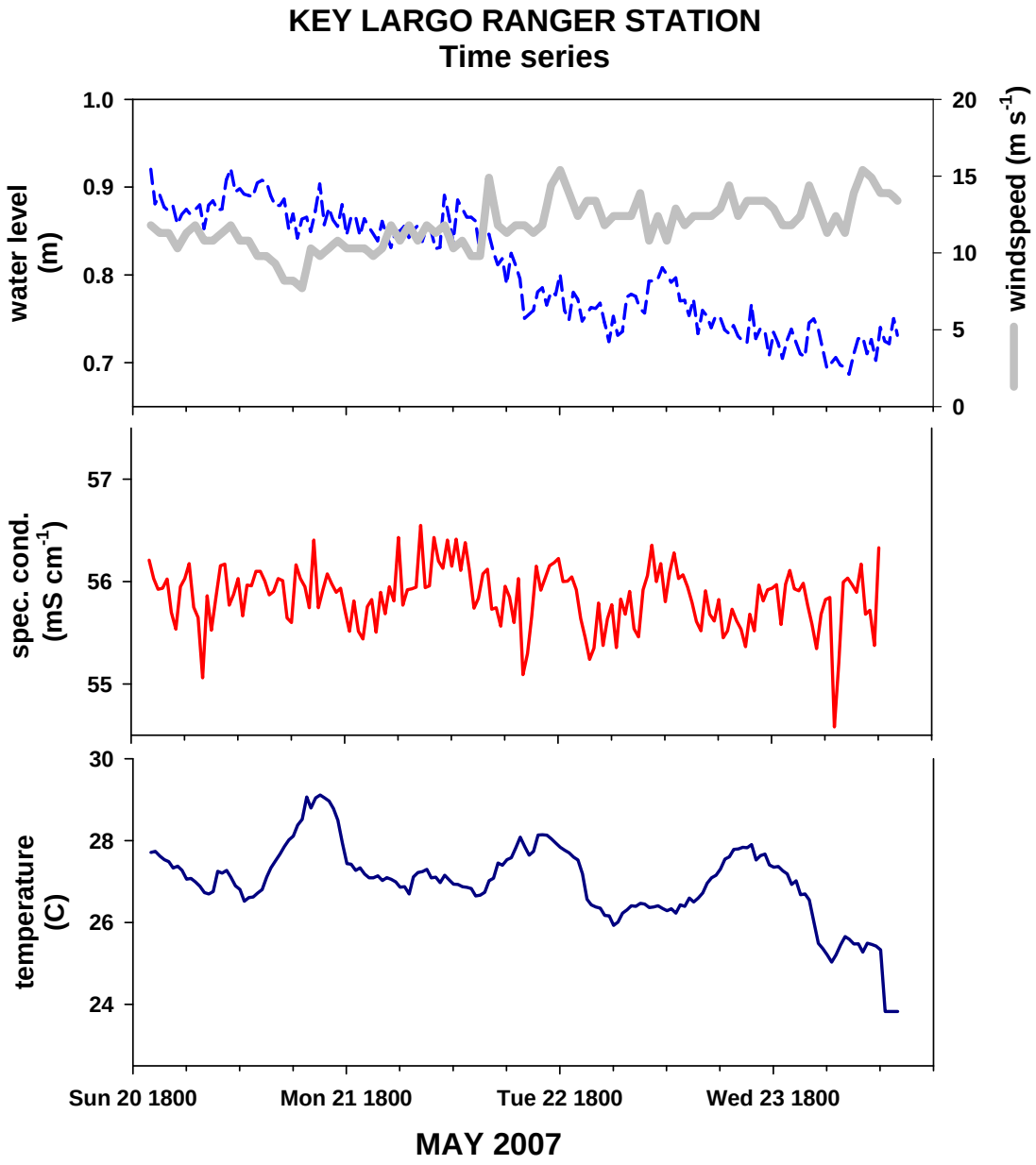

Figure 5. May 2007 time-series water levels (dashed blue line; m), wind speed (solid grey line; m s^{-1}), specific conductivity (mS cm^{-1}), and temperature (^{o}C), Florida Bay.

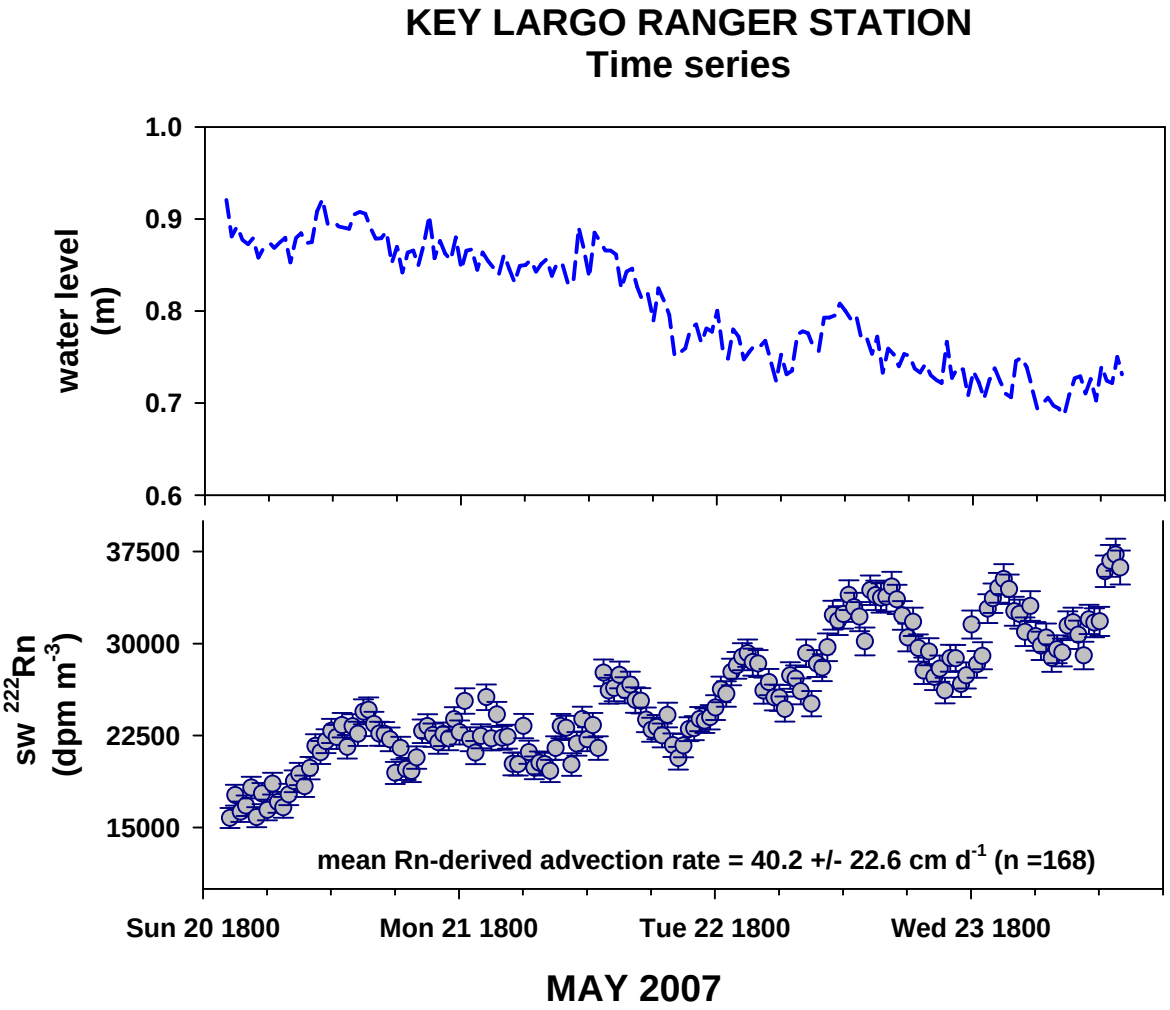

Figure 6. May 2007 time-series water levels (m) and surface water (sw) ^{222}Rn (dpm m^{-3}).

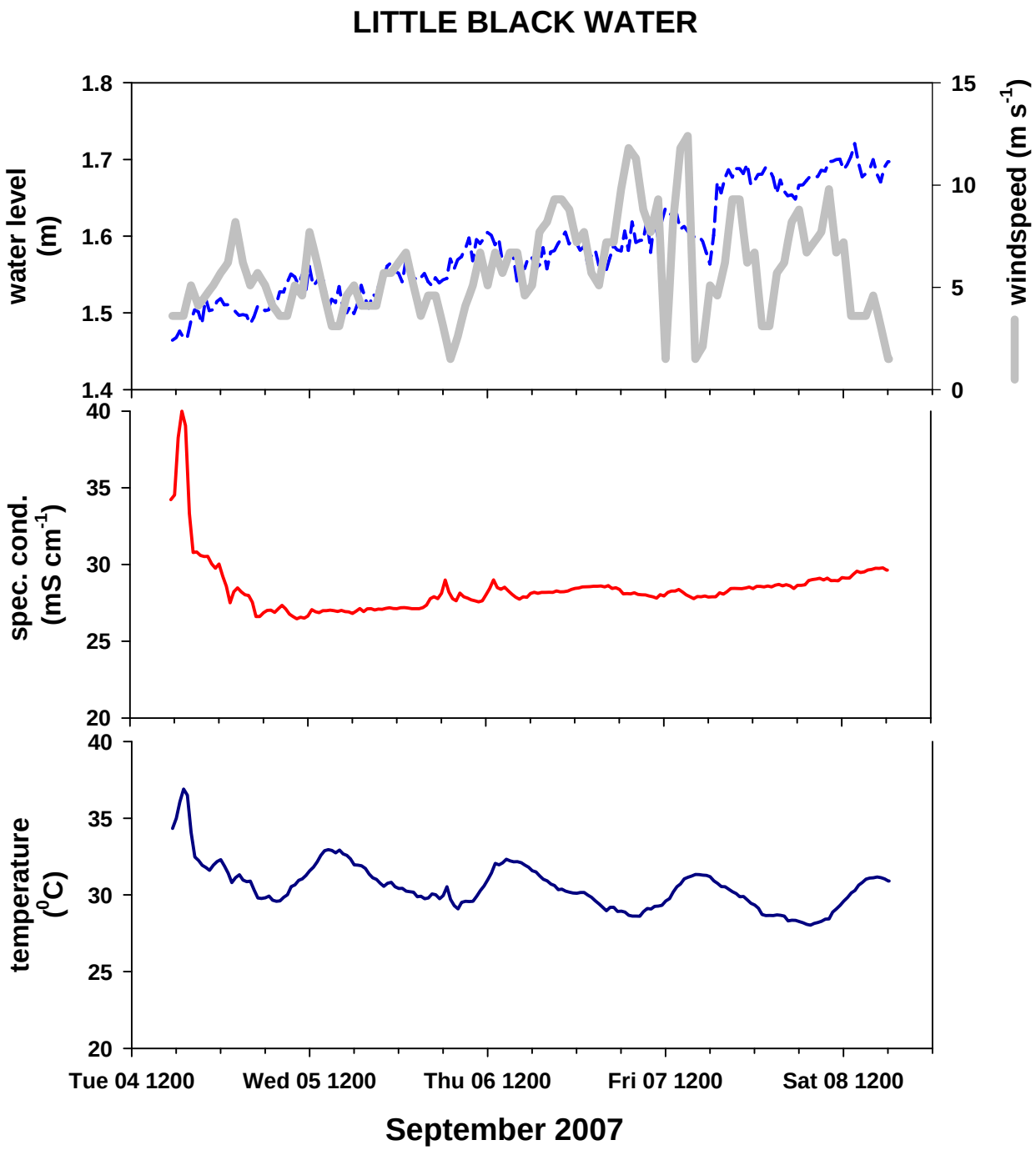

Figure 7. September 2007 time-series water levels (dashed blue line; m), wind speed (solid grey line; m s^{-1}), specific conductivity (mS cm^{-1}), and temperature (^{o}C).

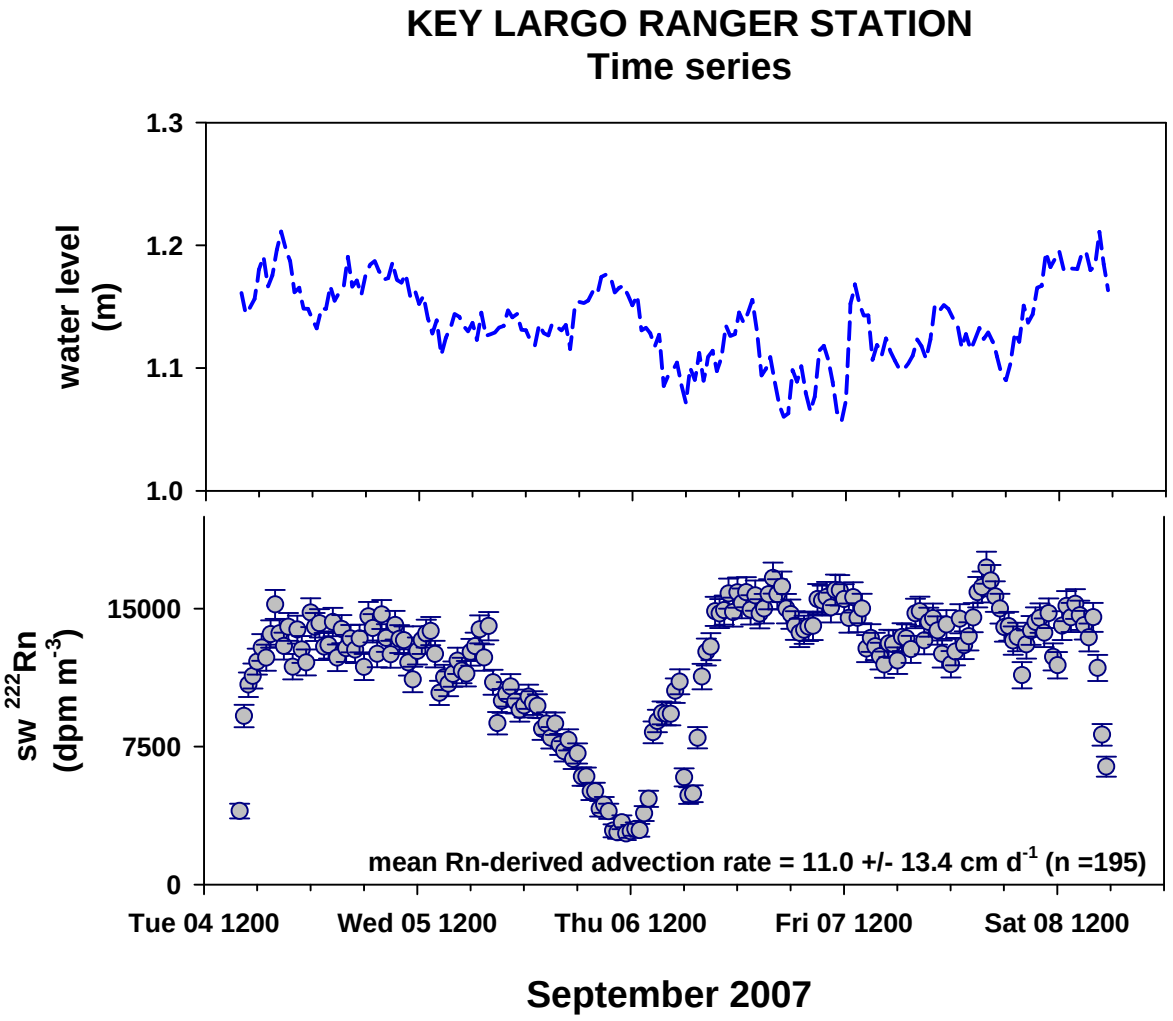

Figure 8. September 2007 time-series water levels (m) and surface water (sw) ^{222}Rn (dpm m^{-3}).

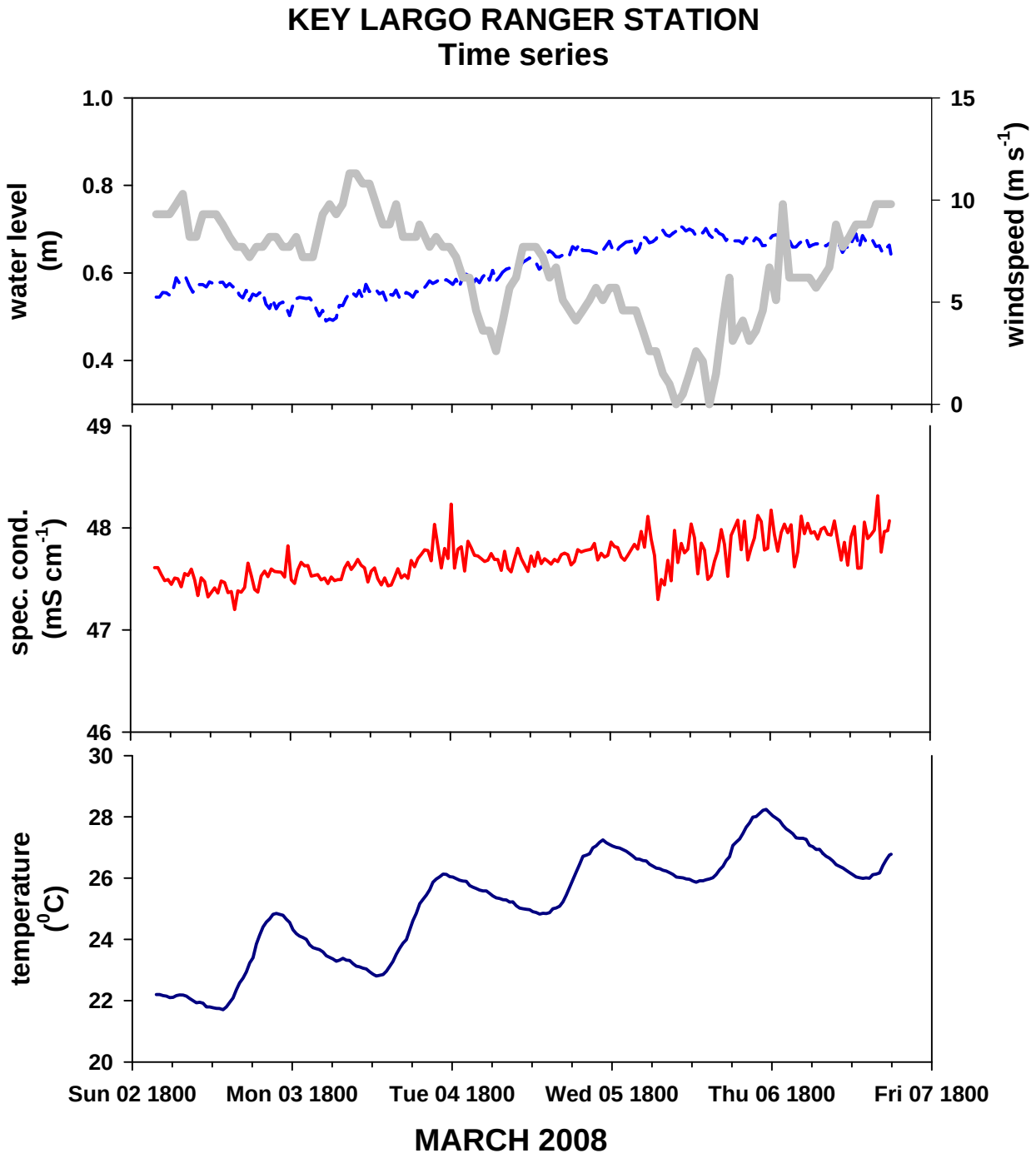

Figure 9. March 2008 time-series water levels(dashed blue line; m), wind speed (solid grey line; m s^{-1}), specific conductivity (mS cm^{-1}), and temperature (^{o}C).

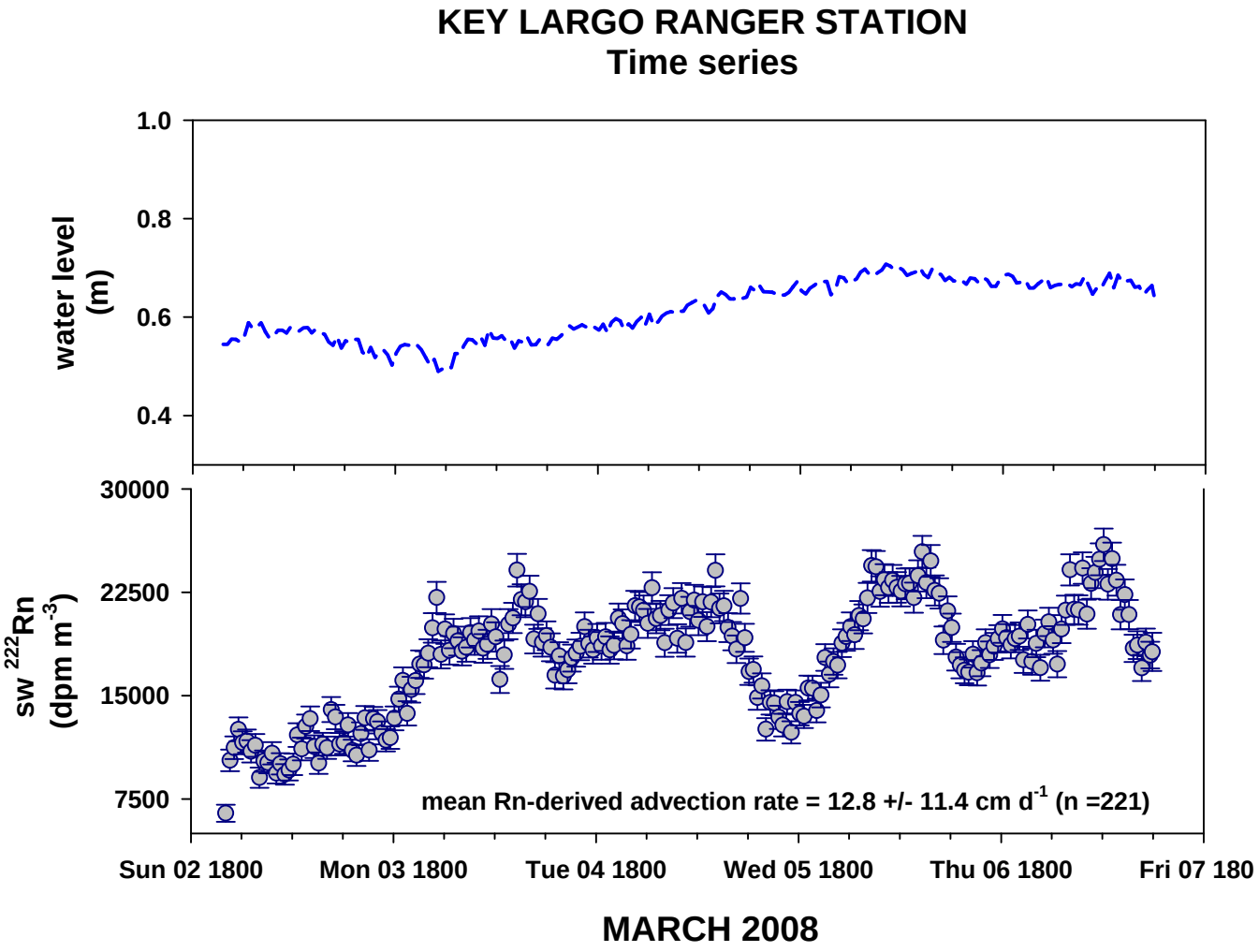

Figure 10. March 2008 time-series water levels (m) and surface water (sw) ^{222}Rn (dpm m^{-3}).

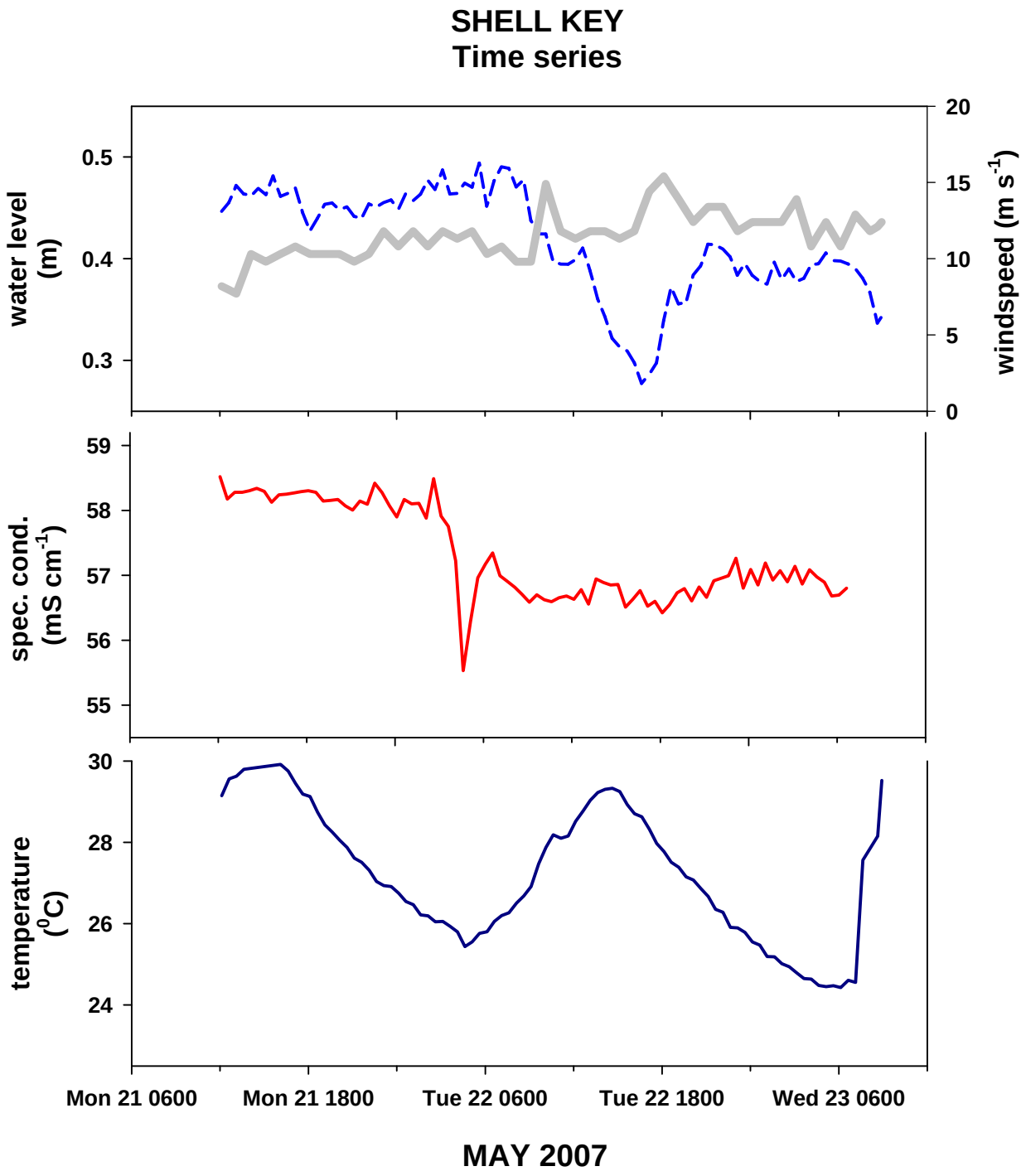

Figure 11. May 2007 time-series water levels (dashed blue line; m), wind speed (solid grey line; m s^{-1}), specific conductivity (mS cm^{-1}), and temperature (^{o}C).

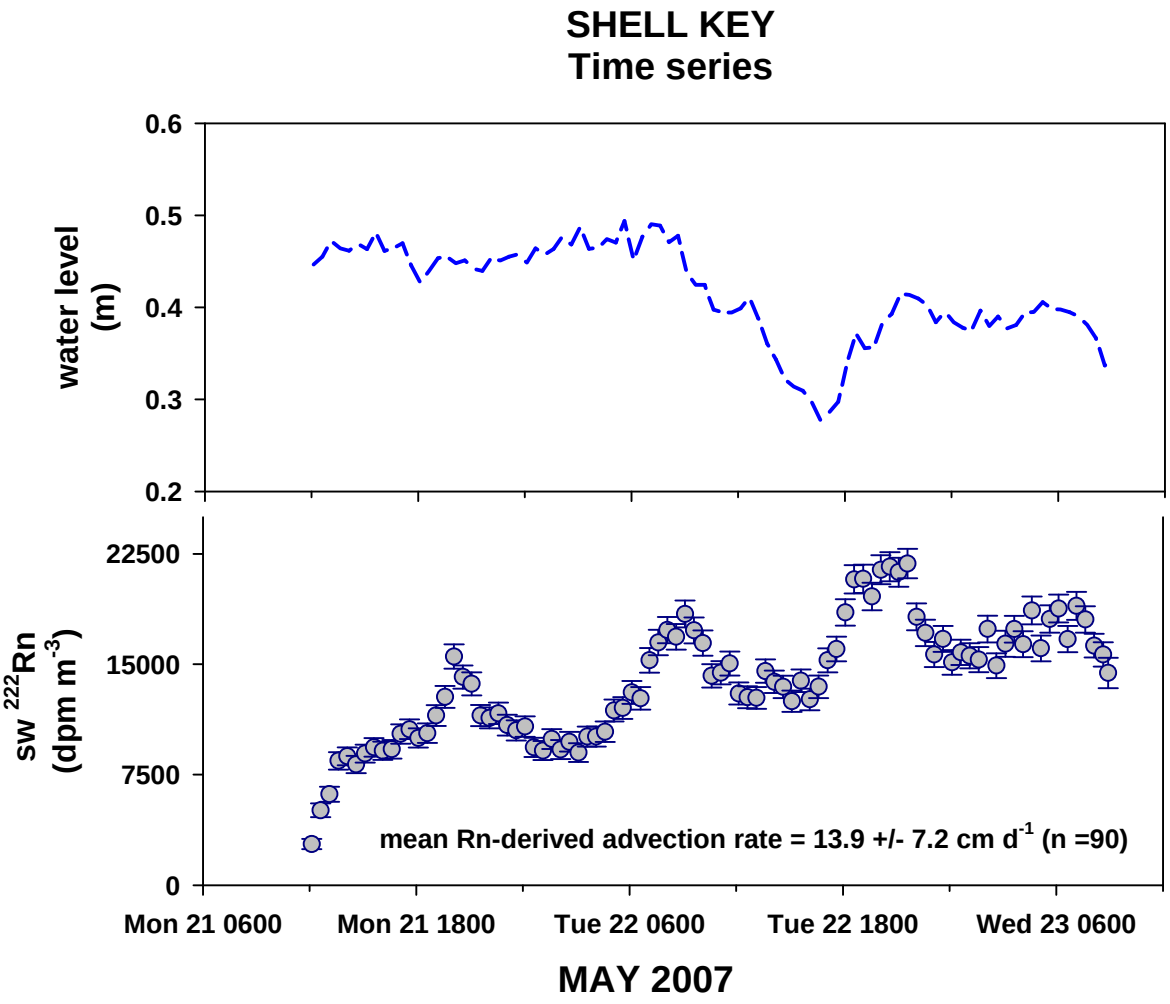

Figure 12. May 2007 time-series water levels (m) and surface water (sw) ^{222}Rn (dpm m^{-3}).

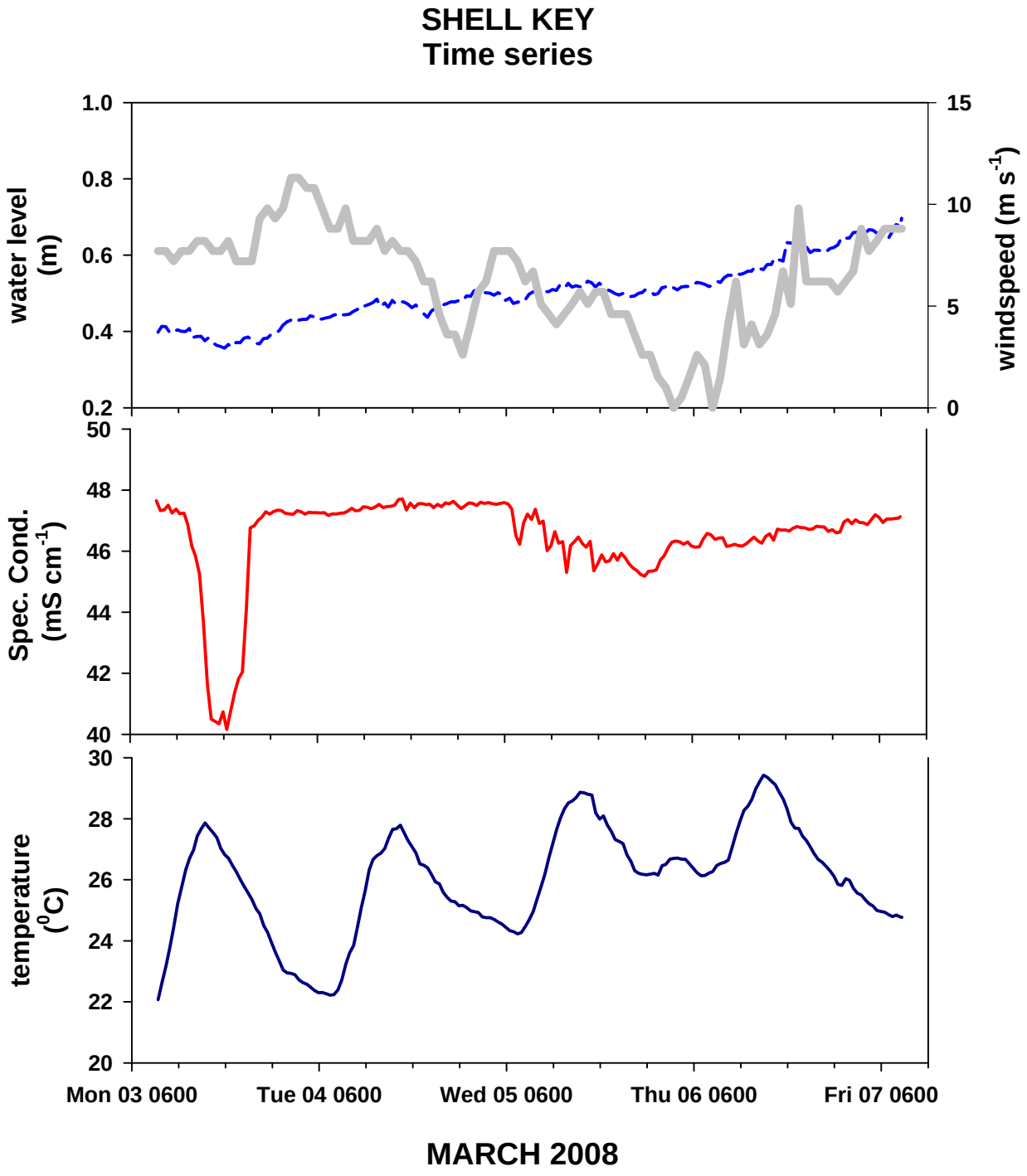

Figure 13. March 2008 time-series water levels (dashed blue line; m), wind speed (solid grey line; m s^{-1}), specific conductivity (mS cm^{-1}), and temperature (^{o}C).

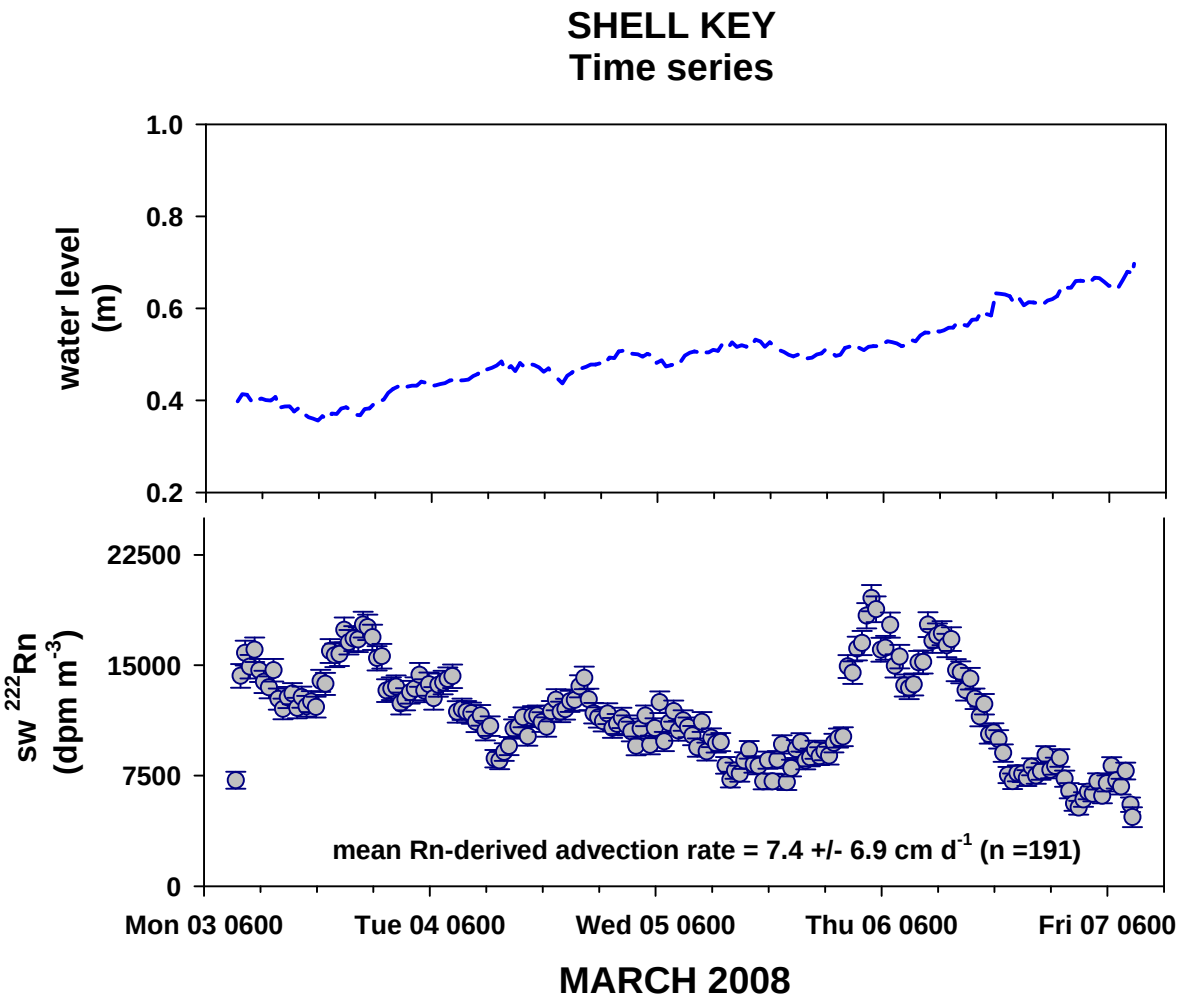

Figure 14. March 2008 time-series water levels (m) and surface water (sw) ^{222}Rn (dpm m^{-3}).

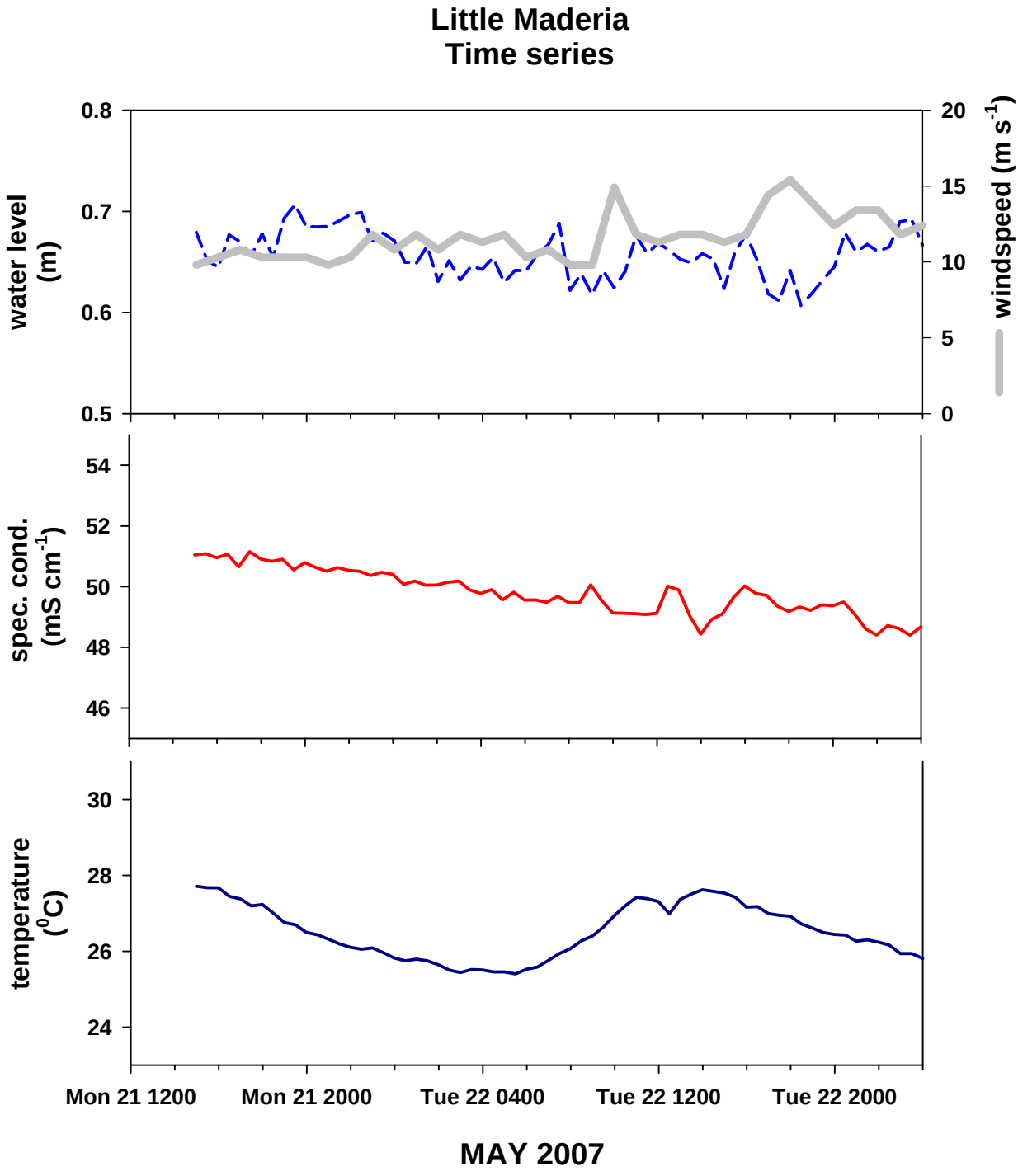

Figure 15. May 2007 time-series water levels (m), wind speed (m s^{-1}), specific conductivity (mS cm^{-1}), and temperature (^{o}C).

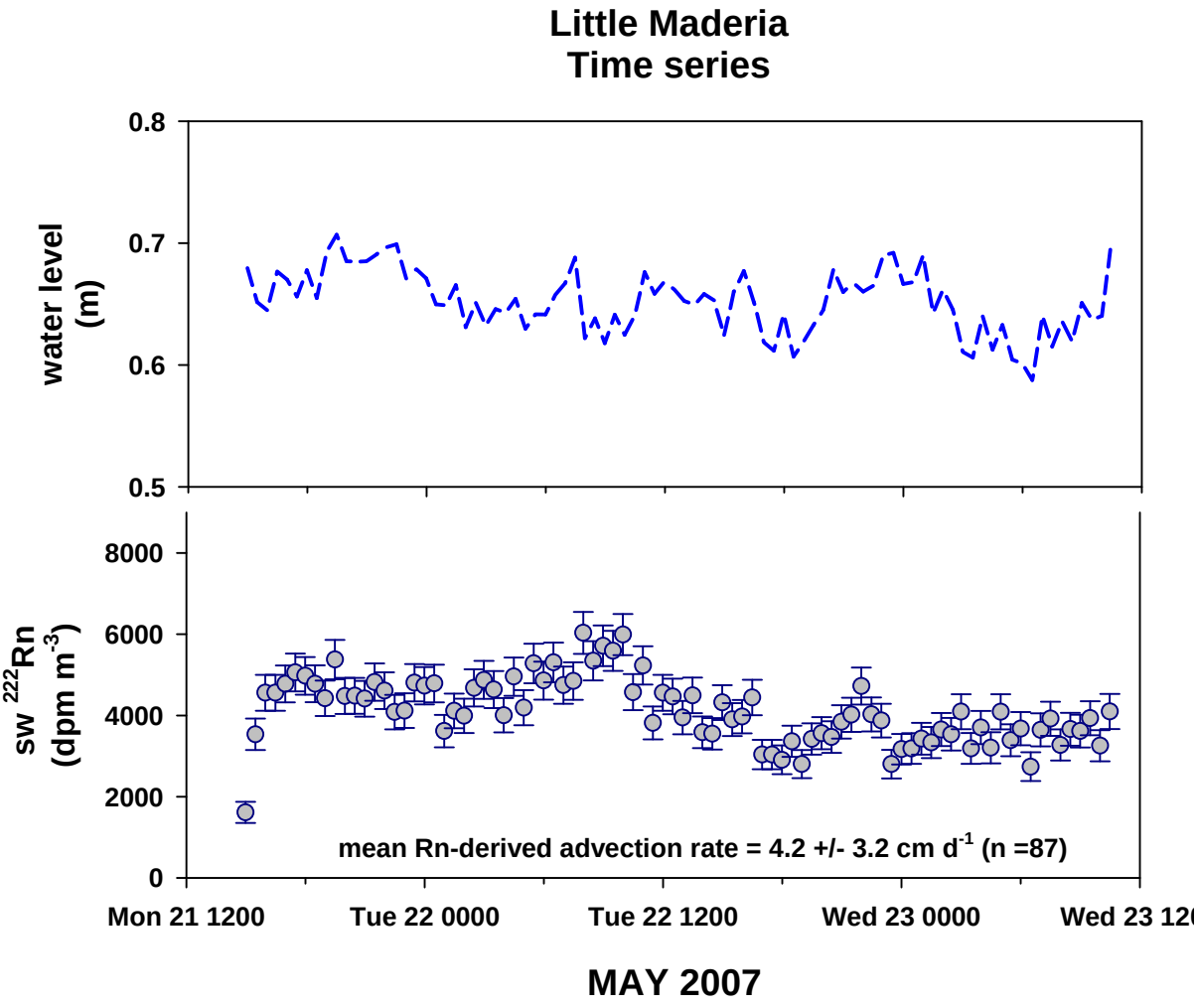

Figure 16. May 2007 time-series water levels (m) and surface water (sw) ^{222}Rn (dpm m^{-3}).

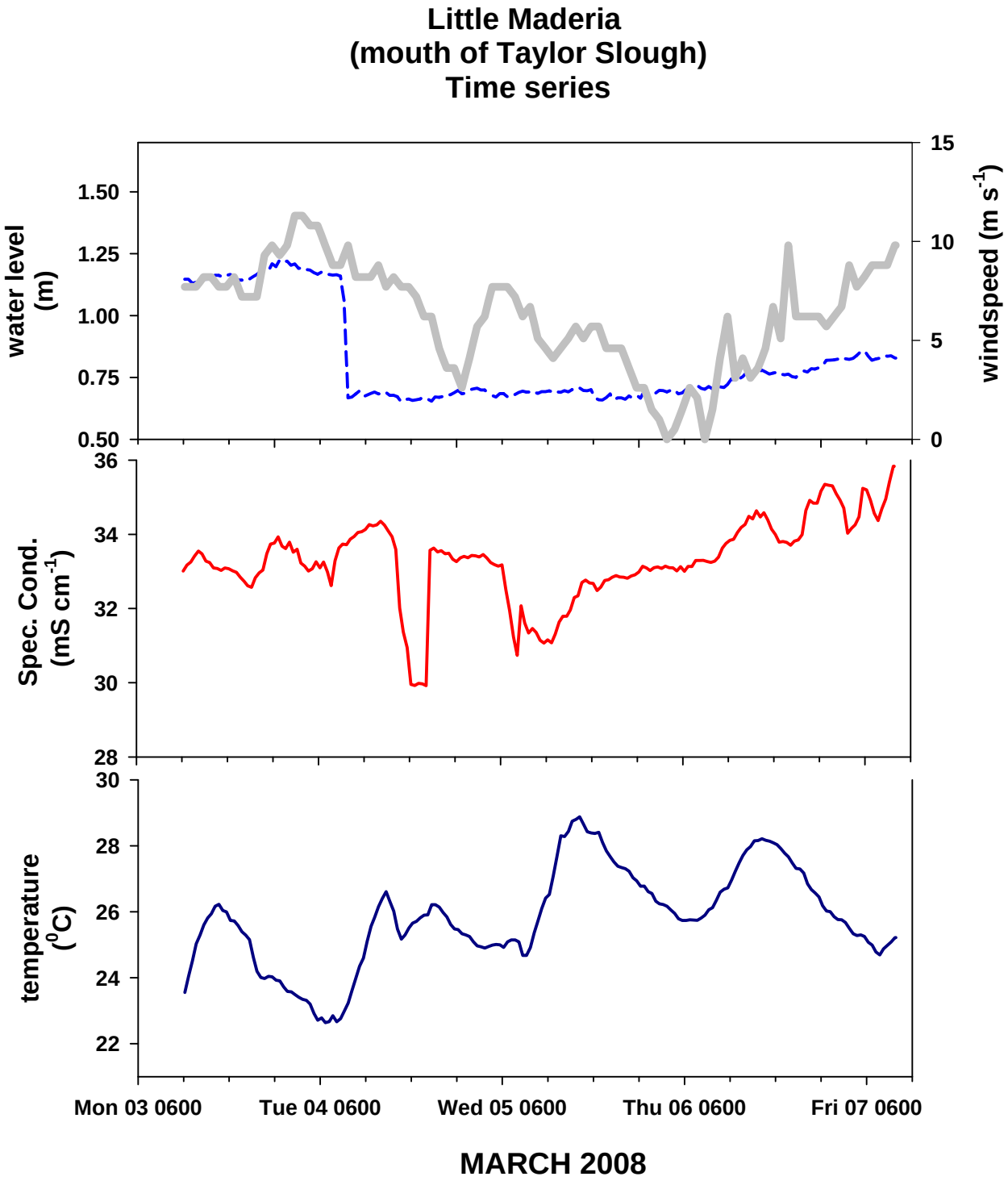

Figure 17. March 2008 time-series water levels (dashed blue line; m), wind speed (solid grey line; m s^{-1}), specific conductivity (mS cm^{-1}), and temperature (^{o}C).

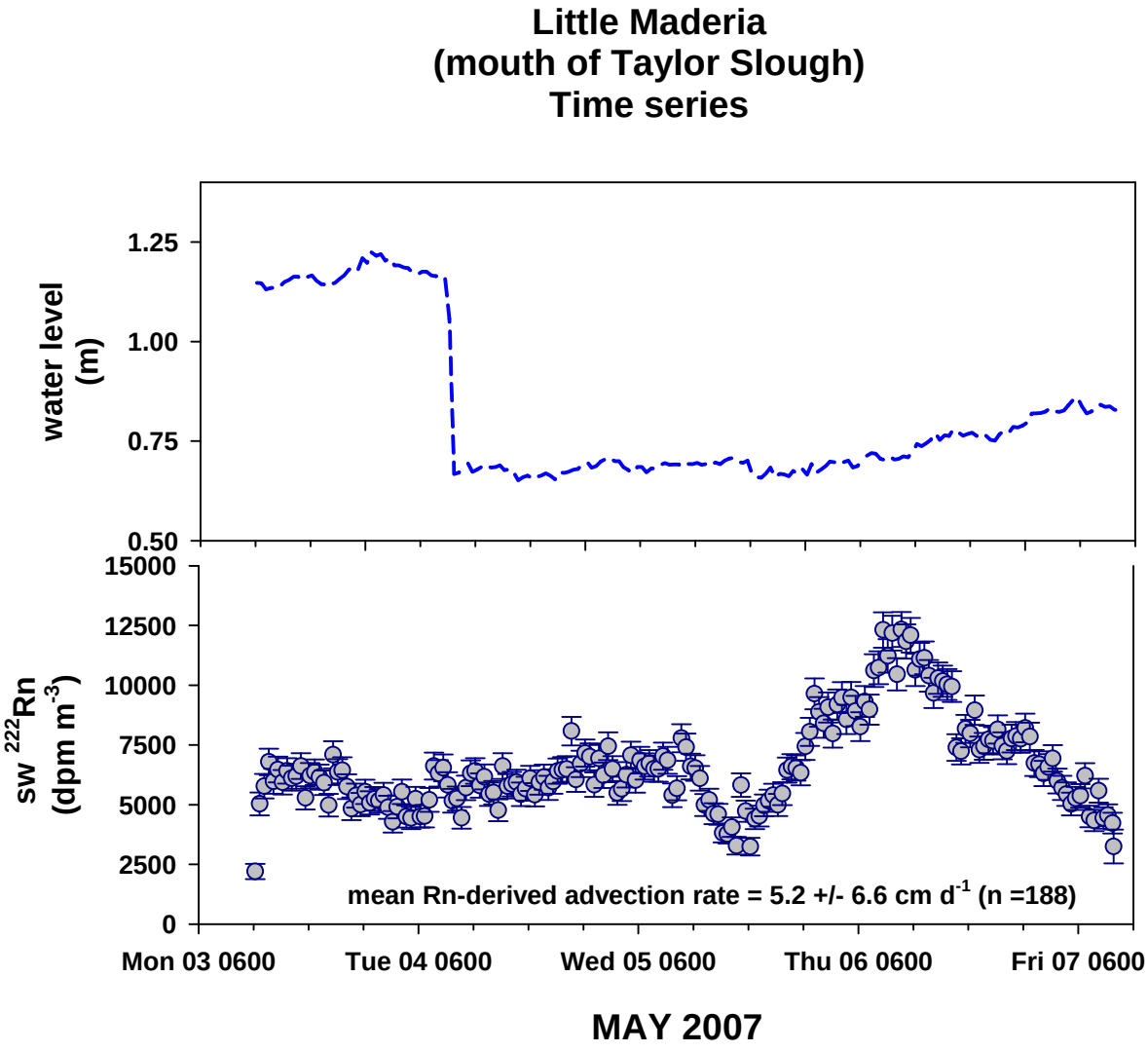

Figure 18. March 2008 time-series water levels (m) and surface water (sw) ^{222}Rn (dpm m^{-3}).

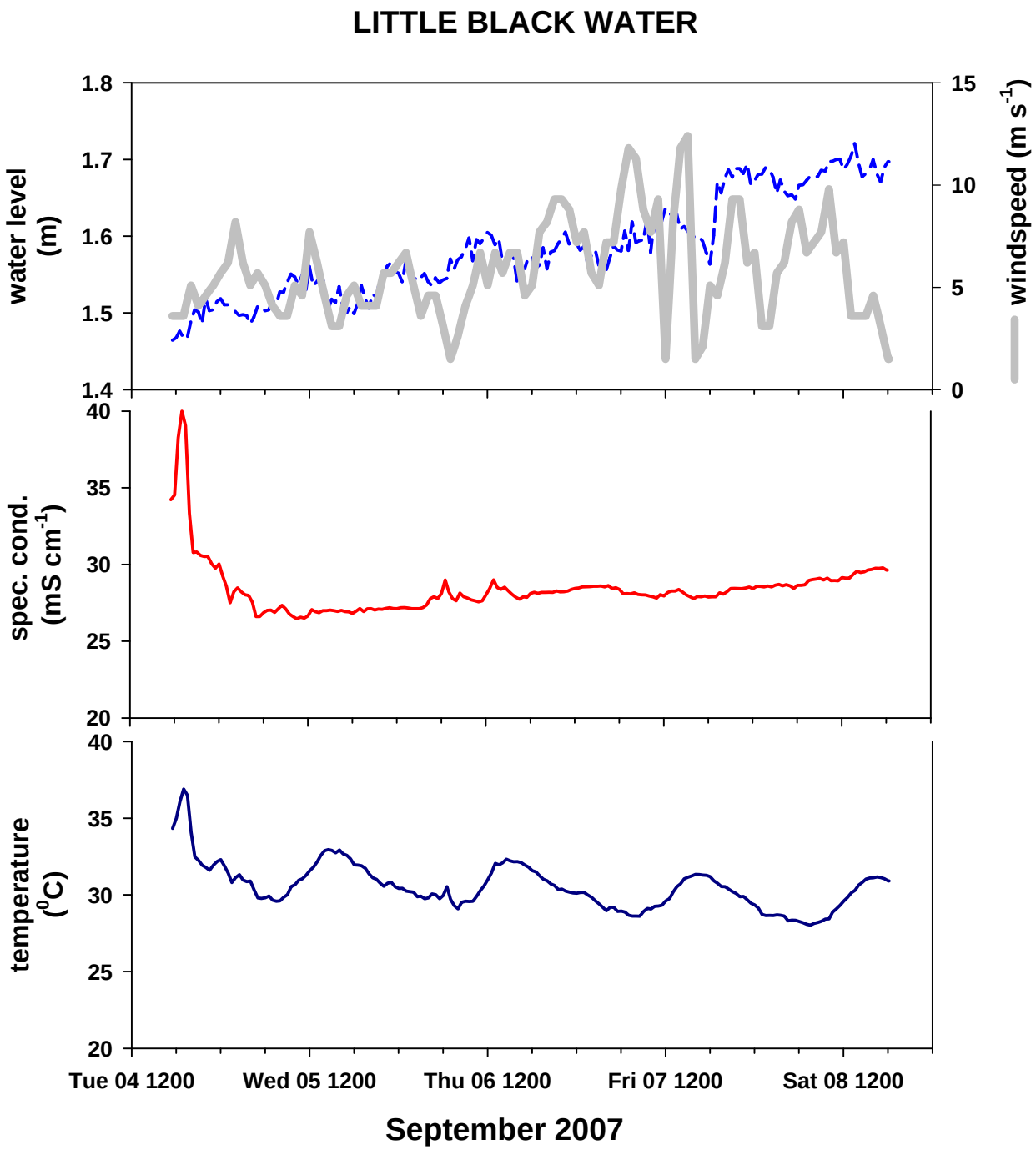

Figure 19. September 2007 time-series water levels (dashed blue line; m), wind speed (solid grey line; m s^{-1}), specific conductivity (mS cm^{-1}), and temperature (^{o}C).

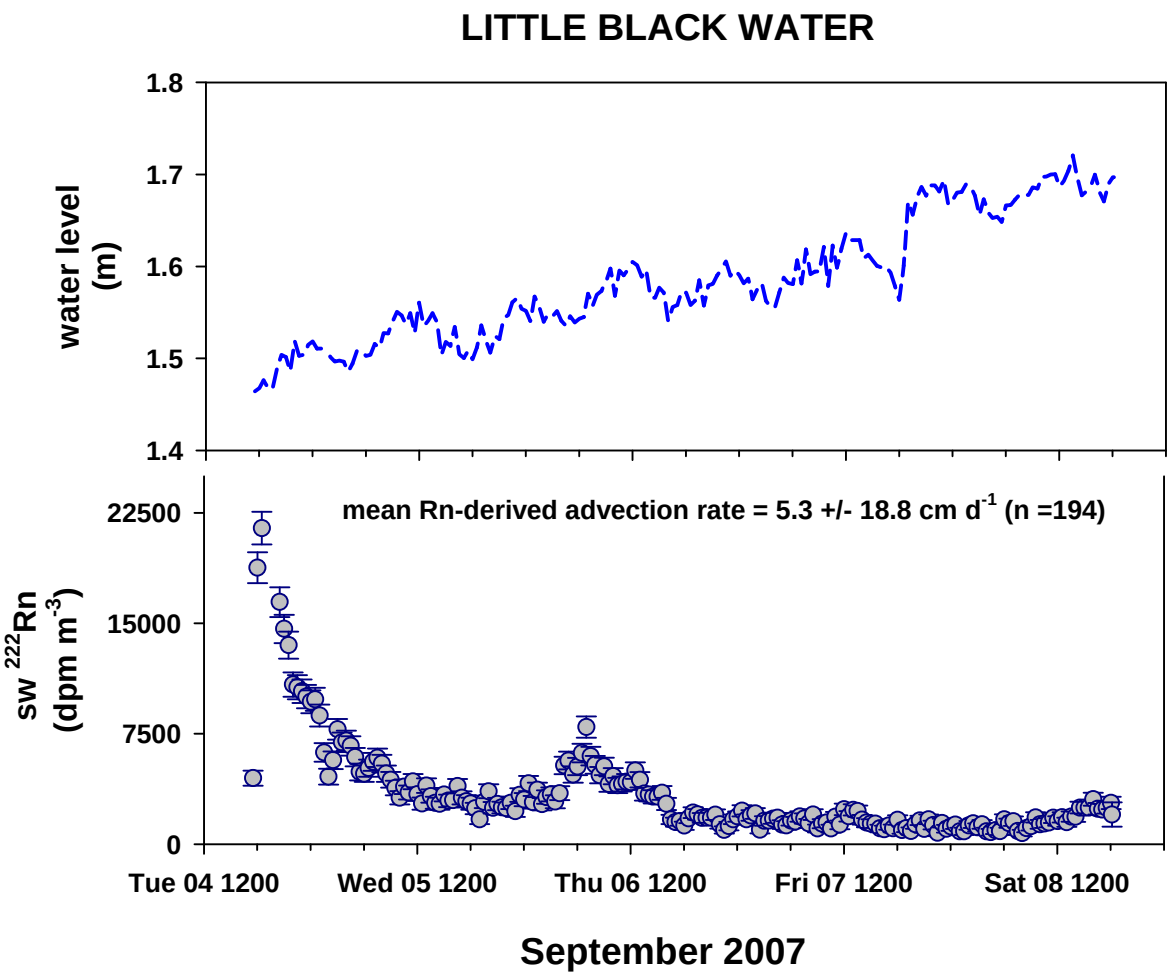

Figure 20. September 2007 time-series water levels (m) and surface water (sw) ^{222}Rn (dpm m^{-3}).

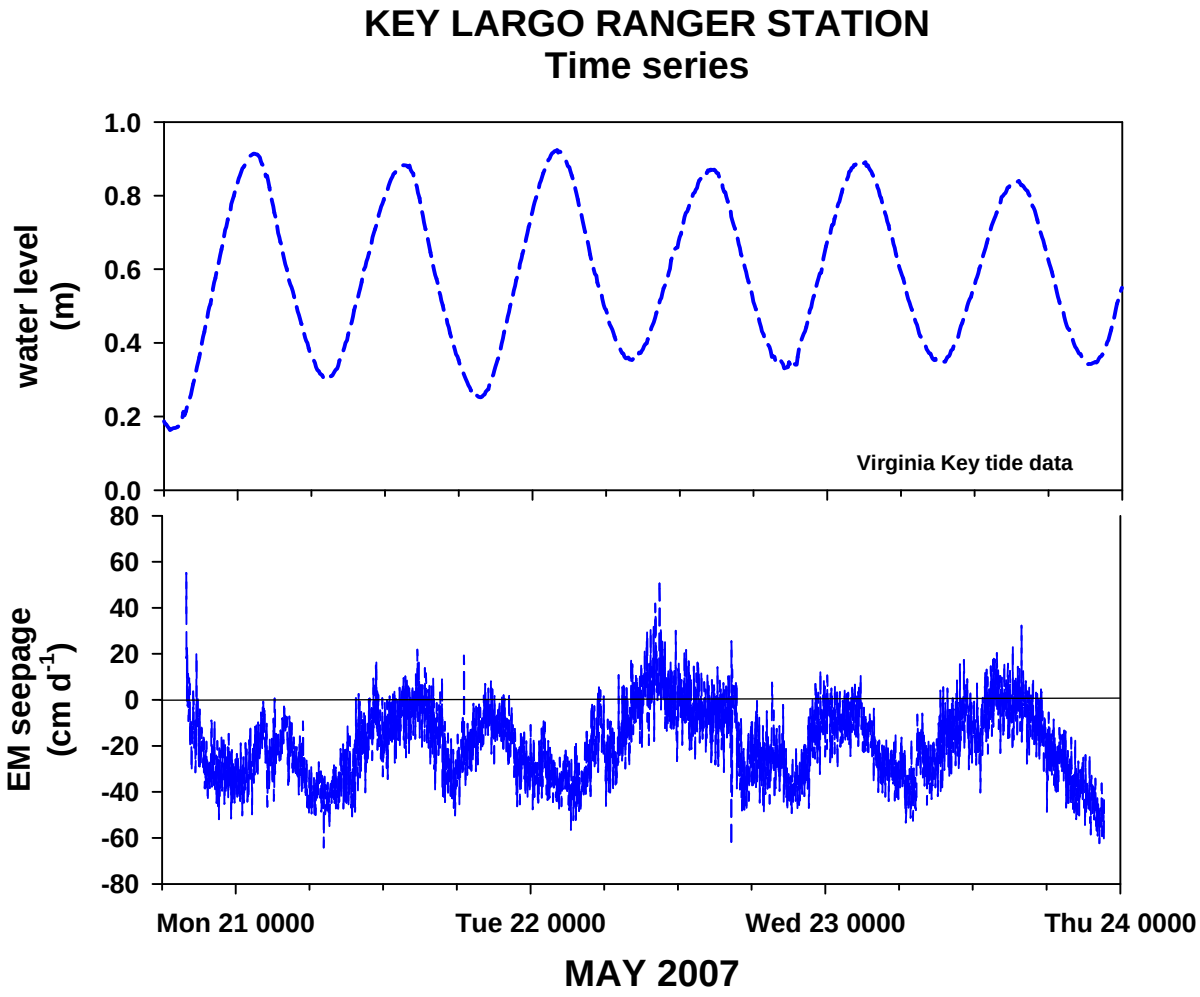

Figure 21. Electromagnetic (EM) seepmeter results during May, 2007.

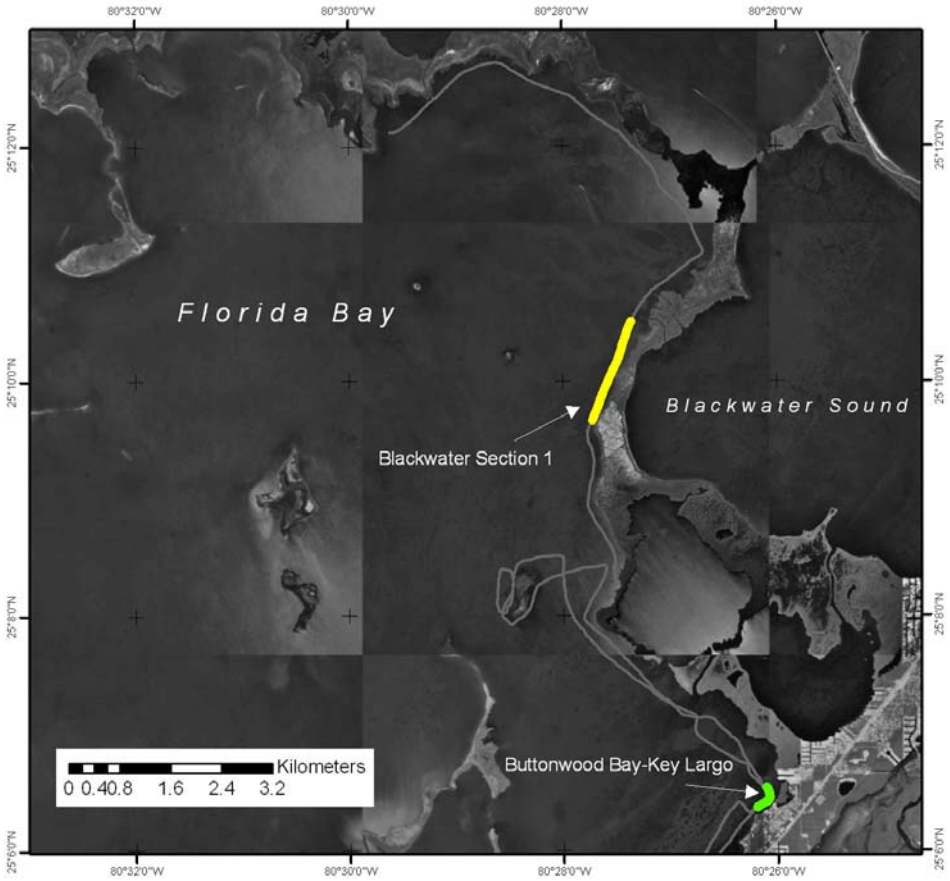

Figure 22. Map showing location of resistivity profiles for Buttonwood Bay-Key Largo and Blackwater Section 1, Florida Bay.

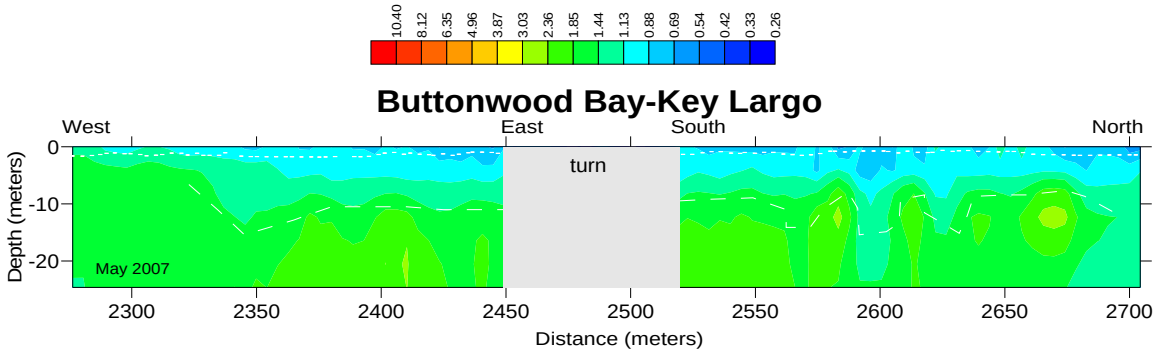

Figure 23. Profile of resistivity behind Key Largo in Buttonwood Sound, Florida Bay, collected in May 2007. Profile shows hummocky nature of subsurface (dashed white line). White line near the surface is the seafloor. Resistivity in ohm-m.

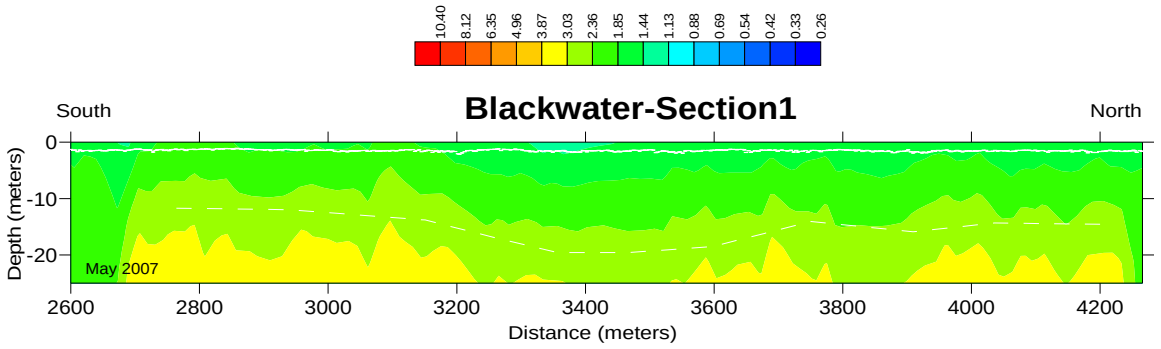

Figure 24. Profile of resistivity along the eastern shore of Florida Bay, opposite of Blackwater Sound. Dip in dashed white line may be representative of lithologic variability. White line near surface is seafloor. Resistivity in ohm-m.

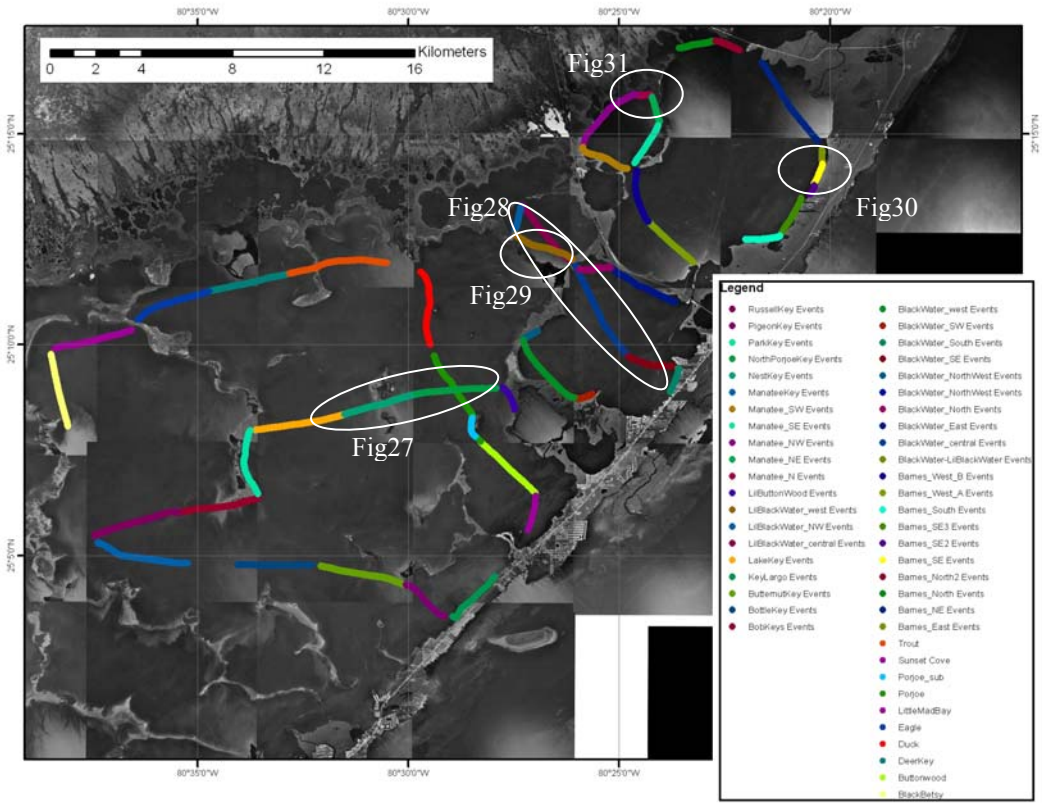

Figure 25. Map showing the resistivity-survey area for September 2007, including the CRP lines and breakdown of individual resistivity profiles.

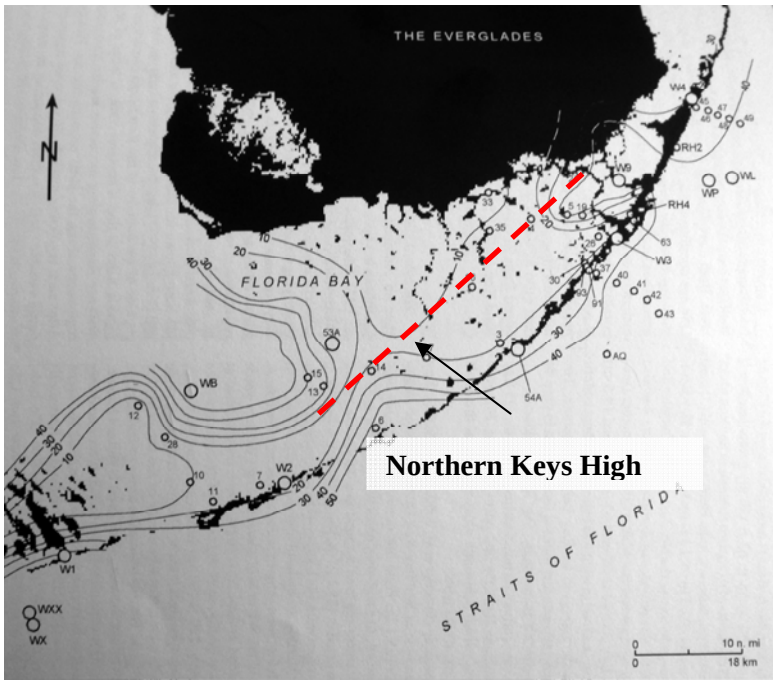

Figure 26. Topography of the Q3 unconformity showing the northern keys high, Florida Bay (modified from Multer et al. 2002).

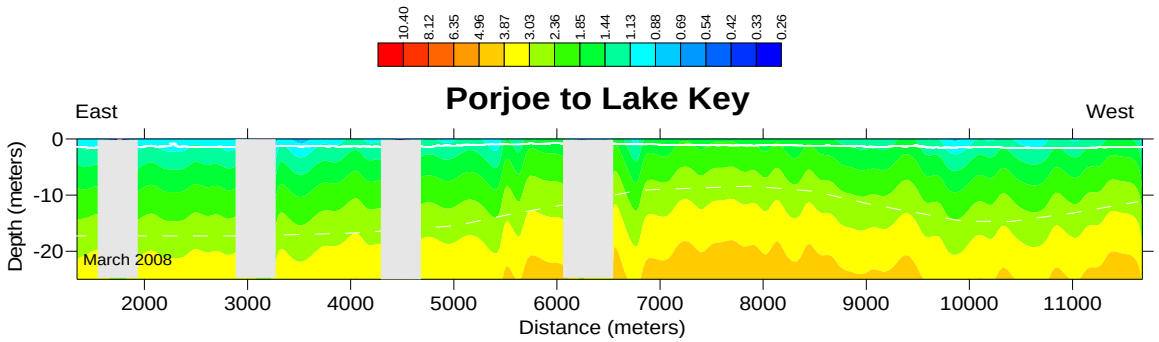

Figure 27. Resistivity profile from east of Porjoe Key west to the eastern side of Lake Key, Florida Bay. The resistivity high that may correspond to a geologic feature known as the Northern Keys High (Multer et al., 2002). Resistivity in ohm-m.

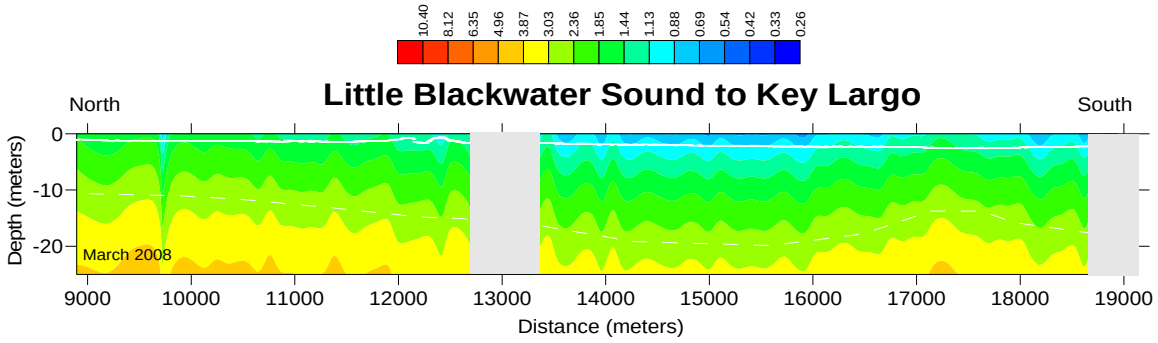

Figure 28. Resistivity profile from Little Blackwater Sound in the north to near Key Largo in Blackwater Soundin the south. T he dip i n re sistivity po ssibly re presents a geologic l ow i n t he m iddle o f Blackwater S ound. Resistivity in ohm-m.

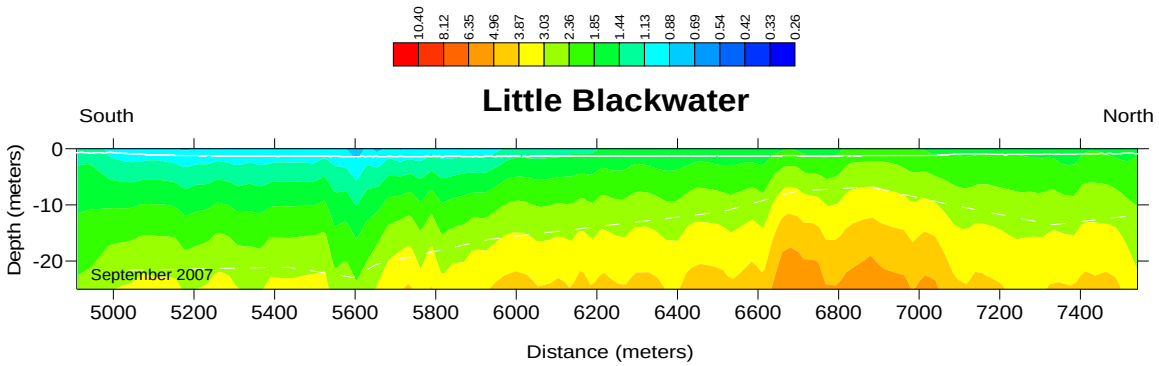

Figure 29. Resistivity section from the southern entrance to Little Black water Sound the mangrove is land that rims the western edge of Little Black water Sound. Increase in resistivity could either be a result of 'fresher' water from the mangrove island to the west or a shallowing of a lithologic unit. Resistivity in ohm-m.

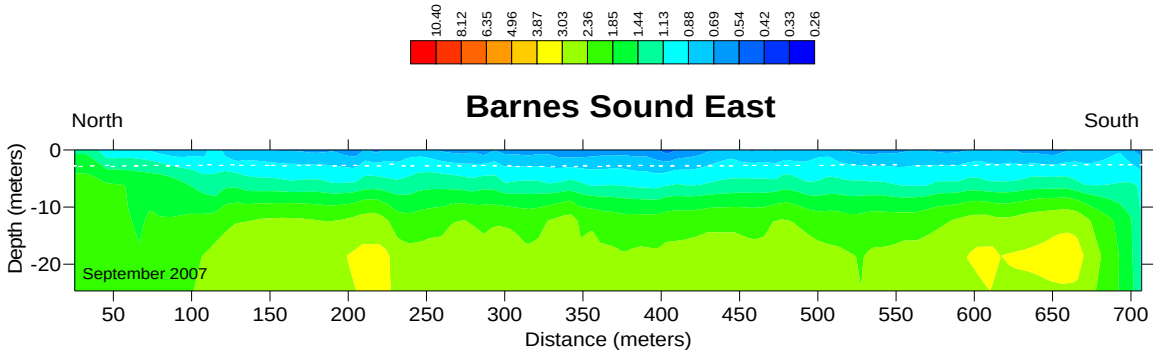

Figure 30. Resistivity profile in BSF, on the bayside of Key Largo. Low resistivity marine water in filled limestone resulting in little variability. Resistivity in ohm-m.

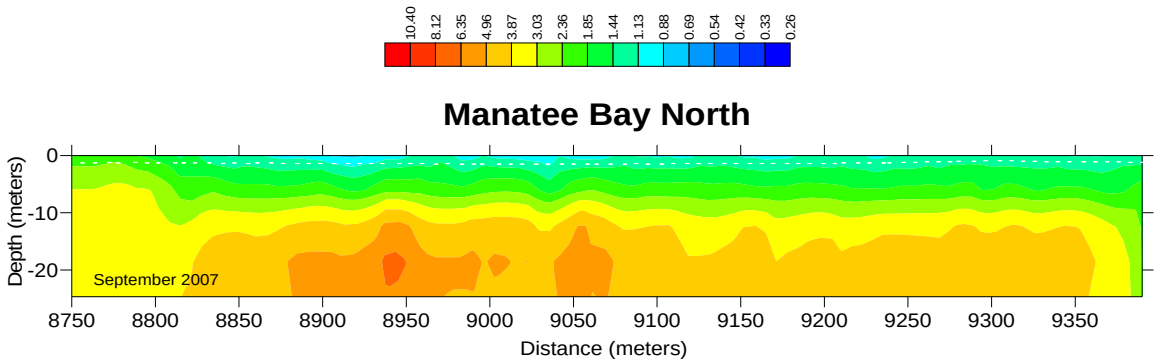

Figure 31. Manatee Bay showing higher resistivity than that found along the backside of Key Largo (FigZ1). The higher resistivity is most likely a response to lower salinity porewaters. Resistivity in ohm-m.

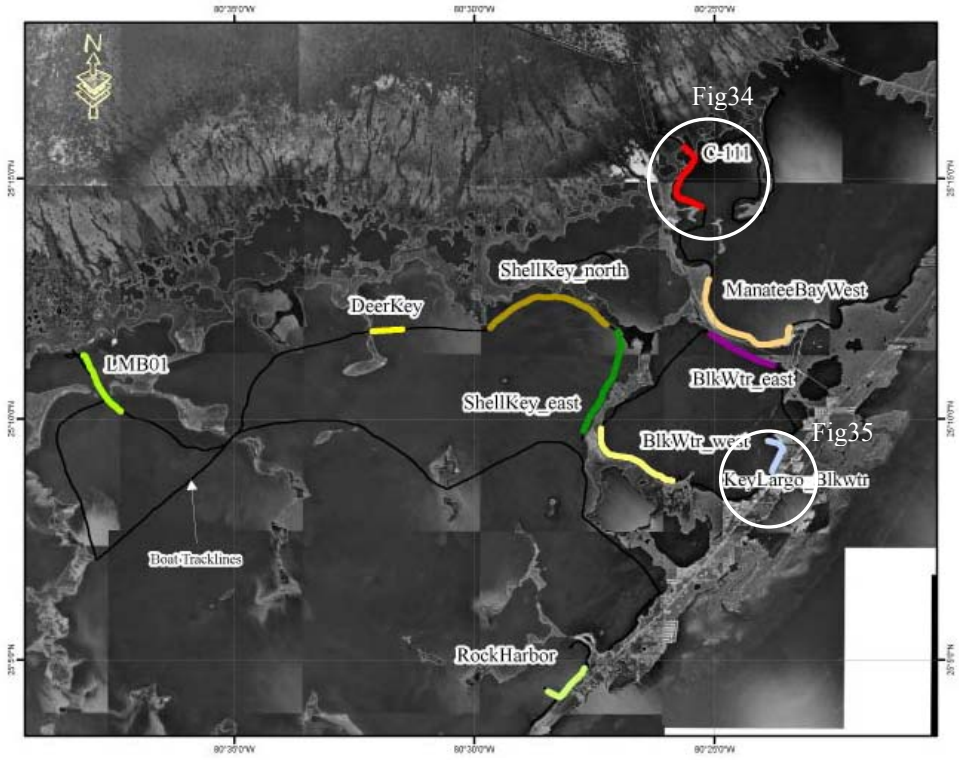

Figure 32. March 2008 boat surveys and respective CRP lines.

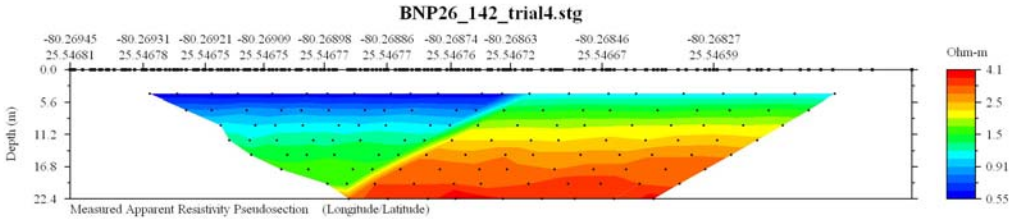

Figure 33. Image of measured (raw) apparent resistivity showing a shift in values between two consecutive data points. It is unknown what causes this shift.

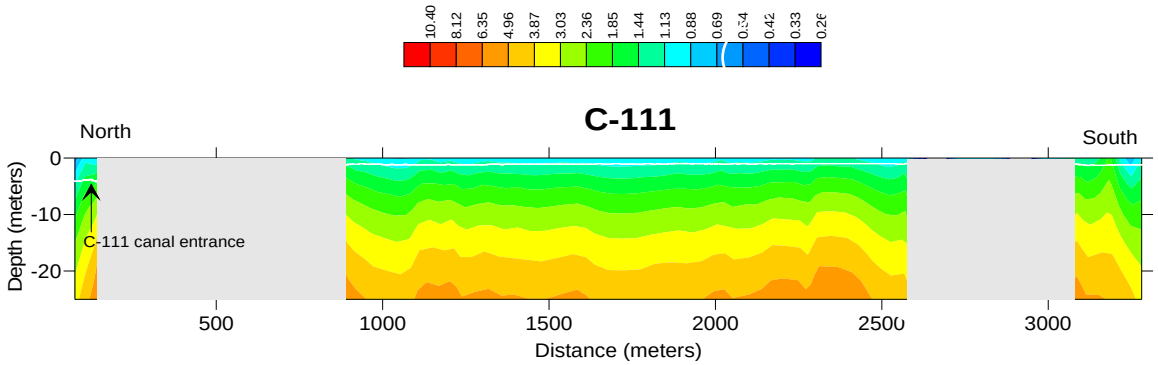

Figure 34. March 2008 CRP profile from within the entrance to C-111 canal out into Manatee Bay, Florida Bay. Profile is typical of previous profiles taken within Manatee Bay. Numerous errors at the beginning of the line are shown by gray boxes. Resistivity in ohm-m.

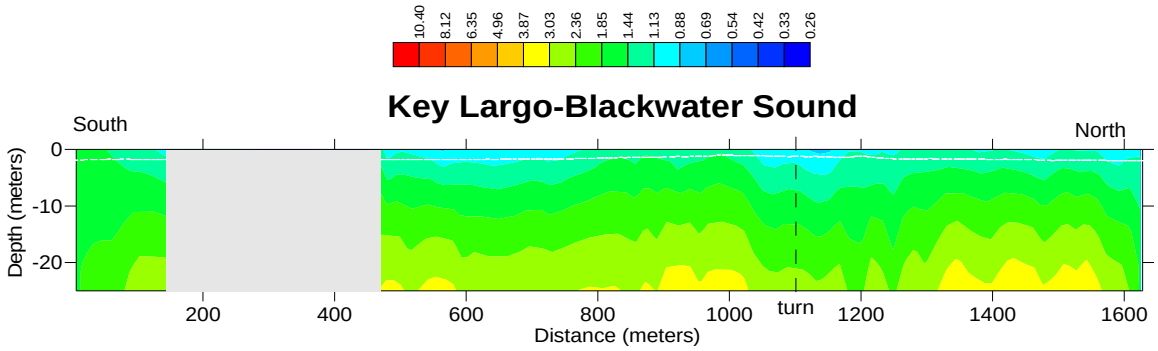

Figure 35. March 2008 CRP profile along the backside of Key Largo in Blackwater Sound. Low resistivity values represent the groundwater exchange of marine salinity due to tidal pumping as well as the representation of slight changes in lithologic composition. Resistivity in ohm-m.